NACA TN 2999

NATIONAL ADVISORY COMMITTEE FOR AERONAUTICS

TECHNICAL NOTE 2999

IMPINGEMENT OF DROPLETS IN 90° ELBOWS WITH POTENTIAL FLOW

By Paul T. Hacker, Rinaldo J. Brun, and Bemrose Boyd

Lewis Flight Propulsion Laboratory
Cleveland, Ohio

Washington
September 1953

NATIONAL ADVISORY COMMITTEE FOR AERONAUTICS

TECHNICAL NOTE 2999

IMPINGEMENT OF DROPLETS IN 90° ELBOWS WITH POTENTIAL FLOW

By Paul T. Hacker, Rinaldo J. Brun, and Bemrose Boyd

SUMMARY

Trajectories were determined for droplets in air flowing through 90° elbows especially designed for two-dimensional potential motion with low pressure losses. The elbows were established by selecting as walls of each elbow two streamlines of the flow field produced by a complex potential function that establishes a two-dimensional flow around a 90° bend. An unlimited number of elbows with slightly different shapes can be established by selecting different pairs of streamlines as walls. The elbows produced by the complex potential function selected are suitable for use in aircraft air-intake ducts.

The droplet impingement data derived from the trajectories are presented along with equations in such a manner that the collection efficiency, the area, the rate, and the distribution of droplet impingement can be determined for any elbow defined by any pair of streamlines within a portion of the flow field established by the complex potential function. Coordinates for some typical streamlines of the flow field and velocity components for several points along these streamlines are presented in tabular form.

INTRODUCTION

As part of a comprehensive research program concerning the problem of ice prevention on aircraft, an investigation of the impingement of cloud droplets on airfoils, aerodynamic bodies, and other aircraft components has been undertaken by the NACA Lewis laboratory. The investigation includes a study of cloud-droplet impingement on low-drag airfoils (refs. 1 to 3) and on cylinders (refs. 4 and 5). Previous investigators have calculated the water-droplet trajectories for cylinders (refs. 6 to 9) and for Joukowski airfoils (refs. 10 and 11). For a complete appraisal of the problem of ice prevention on aircraft, further water-droplet impingement data are needed for aircraft components, including the curved sections or elbows in air-intake ducts.

Icing of air-intake ducts and scoops with subsequent reduction in pressure recovery and in air flow may adversely affect the operation of the aircraft. For example, icing of the air-intake duct for the heat exchanger of a hot-air de-icing system may cause the entire system to fail to provide protection to the aircraft. Curved ducts may also be purposely employed in some applications to act as water-droplet inertia separators to prevent large quantities of water from entering critical components such as carburetors and turbojet engines. The use of a curved duct as a water-droplet inertia separator in the air-intake duct for a carburetor is discussed in reference 12.

In order to prevent or to remove ice formations in curved sections of air-intake ducts or to establish the efficiency of a water-droplet inertia separator, the distribution, the rate, and the extent of droplet impingement must be determined. To obtain these water-droplet impingement data for an airfoil or any other aircraft component such as an elbow, the droplet trajectories with respect to the object must be determined. The droplet trajectories depend upon, among other things, the air-flow field for the component. The flow field for cloud-droplet trajectory studies may be established by one of several methods, such as potential theory or the vortex substitution method, the latter of which makes use of wind-tunnel pressure measurements on the surface of the object. The differential equations that determine the trajectory of a droplet in a curved air stream are highly nonlinear and are most conveniently solved by the use of an analog computer. Because the solution of three-dimensional differential equations by a differential analyzer requires considerably more machine capacity than the same problem in two dimensions, most trajectory studies have been confined to two-dimensional air flows.

The air flow through conventional elbows (constant cross-sectional area) cannot be established by potential theory, and, furthermore, the flow is usually three-dimensional. Therefore, it is difficult to calculate droplet trajectories for conventional elbows. Elbows may be designed, however, for which the flow field is determined by two-dimensional potential theory (ref. 13). For these elbows the pressure losses are usually less than those for conventional elbows of comparable size and shape. (Experimentally determined pressure losses presented in ref. 14 for the basic elbow of this report are about one-third of those for a conventional elbow of comparable size.)

The water-droplet impingement studies presented in this report are for a 90° elbow designed so that the flow field can be obtained by potential theory. The water-droplet impingement data as well as the elbow and flow field are presented in dimensionless form in order that the results be applicable for a wide range of meteorological and flight conditions and sizes and shapes of elbows.

ANALYSIS

Equations of Droplet Motion

As an airfoil or aircraft component moves through a cloud, the interception of cloud droplets by the object is dependent on the physical configuration of the component, the flight conditions, and the inertia of the cloud droplets. In order to obtain the extent of impingement and the rate of droplet impingement per unit area on the component, the cloud-droplet trajectories with respect to the component must be determined. The differential equations that describe the droplet motion in a two-dimensional flow field have been derived in reference 4 and are presented herein in the following form:

$$\left.\begin{aligned} \frac{dv_x}{d\tau} &= \frac{C_D Re}{24}\frac{1}{K}(u_x - v_x) \\ \frac{dv_y}{d\tau} &= \frac{C_D Re}{24}\frac{1}{K}(u_y - v_y) \end{aligned}\right\} \tag{1}$$

where

$$K = \frac{2}{9}\frac{\rho_w a^2 U}{\mu l} \tag{2}$$

and the Reynolds number Re is obtained in terms of the free-stream Reynolds number

$$Re_0 = \frac{2a\rho_a U}{\mu} \tag{3}$$

so that

$$\left(\frac{Re}{Re_0}\right)^2 = (u_x - v_x)^2 + (u_y - v_y)^2 \tag{4}$$

(All symbols are defined in appendix A.)

The differential equations (1) state that the motion of a droplet is governed by the droplet momentum and the drag forces imposed on the droplet by the relative motion between the droplet and the air moving along the streamlines through the elbow. The droplet momentum tends to keep the droplet moving in a straight path, while the drag forces tend to force the droplet to follow the streamline. For very small droplets

and low speeds, the drag forces are much greater than the inertia forces, and little departure from the streamlines occurs; whereas, for large droplets and high speeds, the inertia forces tend to overcome the drag forces, and the droplets deviate considerably from the streamlines and follow a path more nearly in the direction established by the free-stream velocity. In accordance with equations (1) and the definition of the parameter K in equation (2), for a given size and configuration of elbow, the trajectories depend on the radius of the droplets, the airspeed, the air density, and the air viscosity as first-order variables. The trajectories also depend on the size and geometric configuration of the elbow, since these determine the magnitude of the component velocities, u_x and u_y, of the air everywhere in the flow field inside the elbow.

Criteria for Elbow

The air-flow field and the component air velocities for the elbow studied in this report were not determined for a given elbow, but were determined by establishing from potential theory a two-dimensional flow field that makes a 90° turn. Two of the streamlines were selected as walls of an elbow. Several complex potential functions exist that establish the flow around a corner; but, for various reasons, not all these functions are suitable for the design of an elbow. In order to simplify the problem and to produce an elbow that would approximate a conventional elbow, the selection of a complex potential function for the design of a 90° elbow for this study was based upon the following criteria:

(1) The air flow should be uniform and rectilinear at some point before and after the bend, in order that the elbow may be fitted to straight ducts, or, if the elbow is used as a ram scoop with an inlet velocity ratio equal to unity, the entrance flow conditions be provided by the free-stream flow field.

(2) The flow field should be symmetrical with respect to the bisector of the angle of bend of the elbow.

(3) The resultant velocity at any point inside the elbow should not exceed the velocity U where the flow is uniform and rectilinear.

(4) No streamline should have singular points (0 or ∞ velocity) within the elbow.

Elbow Geometry and Flow Field

A complex potential function that establishes a flow field, a portion of which nearly satisfies all the criteria of the preceding paragraph for a 90° elbow, is given in general form by

$$e^{(i+1)\zeta/l} = e^{(i+1)\omega/lU} + e^{(i-1)\omega/lU} \qquad (5)$$

The use of this complex potential function for the design of elbows for potential flow is discussed in references 13 and 14. Details are given in appendix B for designing an elbow and determining its velocity field and other physical characteristics from equation (5) (required for this droplet impingement study).

A portion of the streamline pattern given by equation (5) is shown in figure 1. The flow field between the two streamlines $\psi = \pi lU/8$ and $3\pi lU/8$ (indicated by heavy lines in fig. 1) exactly satisfies all the assumed criteria for a 90° elbow. The first condition is strictly fulfilled only at infinity, because before and after the deflection the stream approaches uniform and rectilinear motion asymptotically. The flow, however, approaches uniform and rectilinear motion very rapidly before and after the bend. Therefore, the ends of the elbow may be selected at some reasonable distance before and after the bend without serious error (see appendix B). For this droplet impingement study, the ends of the elbow were selected as $\xi = 3\pi l/4$ and $\eta = -3\pi l/4$ (indicated by dashed lines in fig. 1).

Since the flow field between the streamlines $\psi = \pi lU/8$ and $3\pi lU/8$ satisfies the assumed criteria, any pair of streamlines between these two streamlines may be selected as walls of a two-dimensional elbow. However, an elbow defined by these two streamlines is probably the most practical elbow, because, for a given entrance width, the average turning radius is smaller for this elbow than for any elbow defined by a pair of streamlines between the two. (See appendix B for definitions of turning radius and elbow entrance width and their relation to the linear parameter l of equation (5). The parameter l determines the size of the elbow.) Therefore, for this droplet impingement study, the elbow defined by $\psi = \pi lU/8$ and $3\pi lU/8$ with ends at $\xi = 3\pi l/4$ and $\eta = -3\pi l/4$ is considered as the basic elbow; and all others, defined by other streamlines, will be considered as supplementary elbows. The droplet impingement calculations will be presented in such a manner, however, that any pair of streamlines between the two basic ones may be chosen as walls of an elbow. The entrance width and average turning radius for the basic elbow are approximately equal to $\pi l/4$ and πl (less than 1-percent error), respectively (fig. 1 and appendix B), with the center of turning located at $\xi = 3\pi l/4$ and $\eta = -3\pi l/4$ (point A, fig. 1). The entrance width and turning radius for supplementary elbows may be approximated by equations given in appendix B.

In order to calculate conveniently the droplet impingement data for an elbow over a large range of meteorological and flight conditions as well as elbow size, it is necessary to express the elbow and its velocity field in terms of dimensionless parameters. This end is accomplished by expressing all distances relative to the elbow as ratios to the linear

parameter l, which is proportional to elbow size, and all velocities as ratios to the free-stream velocity U. The method of obtaining the elbow and velocity field from equation (5) in terms of dimensionless parameters is presented in appendix B. The basic elbow with some typical air streamlines (supplementary elbow walls) is shown in figure 2 in terms of dimensionless parameters x and y. The origin of the coordinate system of figure 2 was translated as compared with figure 1 so that the elbow is entirely in the first quadrant. This translation was made in order to facilitate droplet-trajectory calculations with the analog computer. The relations between the coordinate systems of figures 1 and 2 are

$$\left.\begin{aligned} x &= \frac{\xi}{l} + 1.2 \\ \text{and} \qquad y &= \frac{\eta}{l} + 2.4 \end{aligned}\right\} \tag{6}$$

which place the point of intersection of the streamline $\psi = 3\pi lU/8$ and the elbow entrance (fig. 2) at $x = 0.02185$ and $y = 0.04381$.

The velocity field for the basic elbow is presented in figure 3 in terms of dimensionless parameters. In figure 3(a), the x-component of velocity u_x is given as a function of x for constant values of y, and in figure 3(b), the y-component of velocity u_y is given as a function of y for constant values of x. The component velocities, u_x and u_y, are dimensionless and are equal to the ratio of the actual component velocity to the free-stream velocity U.

An elbow designed by the use of equation (5) may have any entrance cross-section configuration. The only conditions that must be satisfied are (1) the streamlines that form the walls of the elbow at the entrance must remain on the walls throughout the elbow, and (2) the streamlines that form the walls of the elbow are identical to or lie within those defining the basic elbow (fig. 2). Some typical cross sections at various locations through two elbows, one with a rectangular and the other with a circular entrance cross section are shown in figure 4 and discussed in appendix B. The locations of these cross sections are shown in figure 2. The rectangular section is the most convenient elbow entrance cross section with respect to the construction and the application of droplet trajectory data to determine the area, the rate, and the distribution of water-droplet impingement. Therefore, the droplet impingement data presented in RESULTS AND DISCUSSION will apply directly to elbows with rectangular entrance cross sections. However, the same droplet impingement data may be used to find the area, the rate, and the distribution of water-droplet impingement for elbows with any entrance cross section. A method for applying the results to nonrectangular entrance cross sections is outlined in appendix C.

METHOD OF SOLUTION

The differential equations of motion of a droplet in a two-dimensional flow field are difficult to solve by ordinary means, because the values of the component relative velocity between air and droplet, required to solve equations (1), are functions of the droplet position and velocity, and these are not known until the trajectory is traced. The total relative velocity at each position is also required in order to determine the value of the local Reynolds number (eq. (4)). The value of C_D as a function of Re for the droplets, required in equations (1), was taken from tables in reference 7. Simultaneously, solutions for the two equations were obtained with a mechanical analog constructed at the Lewis laboratory for this purpose (ref. 4). The results were in the form of plots of droplet trajectories with respect to the elbow.

The equations of motion (eq. (1)) were solved for the following six values of the inertia parameter K: 1/6, 1/3, 4/7, 1, 2, and 4. For each value of K, a series of trajectories was computed for each of four values of free-stream Reynolds number Re_0: 0, 32, 128, and 512. The end of the elbow nearest the origin of figure 2 was chosen as the entrance. Trajectories were computed for the various combinations of K and Re_0 for droplets that entered the elbow at several positions across the elbow.

Assumptions necessary to the solution of the problem are:

(1) The droplets enter the elbow with the same velocity as the air (fig. 3).

(2) The droplets are always spherical and do not change in size.

(3) No gravitational forces act on the droplets.

RESULTS AND DISCUSSION

Method of Presenting Data

The impingement data presented in this section, which apply only to elbows with rectangular entrance cross sections, are divided into two categories: those for the basic elbow (defined by streamlines $\psi = 3\pi lU/8$ and $\pi lU/8$) and those for any supplementary elbow defined by any pair of streamlines between those for the basic elbow (such as $\psi = 5\pi lU/16$ and $3\pi lU/16$). A method is outlined in appendix C for extending these results to elbows of nonrectangular entrance cross sections.

For convenience in presenting and discussing the impingement results, the wall with the largest value of ψ is designated as the outside wall, and the other as the inside wall. Because of the physical configuration of the elbow (flow field) and the direction of the droplet inertia forces, droplet impingement can occur only on the outside wall of the elbow. The area of impingement on the outside wall starts at the entrance and extends in a downstream direction, the extent depending upon the values of K and Re_0.

In presenting the data, use is made of the abscissa values of streamlines and droplet trajectories at the elbow entrance. In order to differentiate between abscissa values for streamlines and droplet trajectories, the notation adopted herein involves the use of double subscripts for the x-coordinate (illustrated in fig. 5). The first subscript of each pair indicates that the abscissa value refers to a streamline ψ or to a droplet trajectory d. The second subscript refers to a particular streamline or droplet trajectory; for example, o refers to outside wall, and m refers to the maximum initial value of abscissa of droplets that impinge in the elbow. The omission of the second subscript indicates that the quantity is a variable. All symbols having a prime superscript refer to the basic elbow, whereas unprimed ones refer to supplementary elbows.

An analysis of the series of droplet trajectories computed for the basic and supplementary elbows showed that all the important information necessary to calculate the extent, the rate, and the distribution of droplet impingement could be summarized in terms of

(1) Entrance width of elbow being considered

(2) Distance along outside wall S from entrance of elbow to point at which droplet trajectory meets wall (some lines of constant distances and some typical trajectories are shown in fig. 2 for basic elbow and intermediate streamlines; S is dimensionless and has the same dimensionless scale as x)

(3) Abscissa value of droplet trajectories at elbow entrance (x_d for basic elbow)

(4) Values of dimensionless parameters K and Re_0

Presentation of impingement data in terms of the dimensionless parameters K and Re_0 is very convenient, but the physical significance of these parameters is often obscure unless use is made of their definitions (eqs. (2) and (3)). In order that these dimensionless parameters have some physical significance in the following discussion, some typical combinations of K and Re_0 are presented in table I in terms of elbow size, droplet size, free-stream velocity, air density, and air viscosity.

Basic Elbow

The droplet trajectory information required to calculate the extent, the rate, and the distribution of droplet impingement for the basic elbow is summarized for various combinations of K and Re_0 in figure 6. This figure is a plot of the distance S' along the outside wall of the elbow from the entrance to the point of impingement of droplets that enter the elbow at various values of x_d'. (The length of the outside wall of the basic elbow is 6.46 S units.) From the data presented in this figure, the extent, the rate, and the distribution of water-droplet impingement can be determined. The data presented in figure 6(a) for $Re_0 = 0$ (Stokes' law) can be considered as a limiting case, since they apply to an ideal situation that cannot be attained in practice. The curves for $K = \infty$ represent a limiting case in which the conditions are such that the droplet trajectories are straight lines parallel to the direction of the free-stream velocity U.

Maximum extent of impingement S_m'. - The maximum extent of impingement for the basic elbow for a given combination of K and Re_0 is determined from figure 6 by the maximum value of S for any value of x_d' within the walls of the elbow. For some combinations of K and Re_0 such as $K = 4/7$ and $Re_0 = 128$ (fig. 6(c)), impingement occurs throughout the entire length of the elbow with some droplets passing through without impinging, as is illustrated in figure 5(a). For other combinations of K and Re_0, such as $K = 2$ and $Re_0 = 32$ (fig. 6(b)), the impingement of all the droplets is confined to a portion of the outside wall, as is illustrated in figure 5(b). The maximum extent of impingement when $K = 2$ and $Re_0 = 32$ (fig. 6(b)) is 4.7 S units. The maximum extent of impingement S_m' is presented in figure 7 as a function of the reciprocal of K for four values of Re_0 and in table I for some typical values of K and Re_0. The value of S_m' varies directly with Re_0 and inversely with K.

Droplet trajectories were computed beyond the exit of the elbow for some combinations of K and Re_0. These extended trajectories were computed for a uniform rectilinear flow field with velocity U such as would be present in a straight duct connected to the elbow. The trajectories of the droplets before emerging at the exit of the elbow were almost parallel to the air streamlines at the exit (fig. 2), and upon entering the uniform flow field of the straight duct the droplet trajectories became so nearly parallel to the streamlines and outside wall that it was difficult to determine the exact point of impingement. Although there is some impingement in the straight duct, the amount of water

impinging per unit area is small, as is discussed in a later section. Since the impingement point in the straight duct was difficult to determine, the data on maximum extent of impingement presented in figures 6 and 7 are terminated at the exit of the basic elbow ($S' = 6.46$).

Collection efficiency E'. - Collection efficiency of the elbow is defined as the ratio of the amount of water impinging within the elbow to the amount of water entering the elbow. If the assumption is made that the water droplets are uniformly dispersed in the air entering the elbow, then the collection efficiency can be expressed in terms of the width of the elbow at the entrance $x'_{\psi,i} - x'_{\psi,o}$ and the difference in abscissa values at the elbow entrance of the two droplet trajectories that define the extent of impingement. The abscissa value of the trajectory that defines the forward boundary of impingement ($S' = 0$), defined as $x'_{d,o}$, has the same value as the outside wall of the elbow $x'_{\psi,o}$ (fig. 5). The abscissa value of the trajectory that defines the rearward extent of impingement, designated as $x'_{d,m}$ (fig. 5), is determined from figure 6 at the maximum value of S' for a given combination of values of K and Re_0. The difference $x'_{d,m} - x'_{d,o}$ is proportional to the amount of water impinging on the elbow wall, and the width of the elbow entrance $x'_{\psi,i} - x'_{\psi,o}$ is proportional to the total amount of water in droplet form entering the elbow. Hence, the collection efficiency E' is given by

$$E' = \frac{x'_{d,m} - x'_{d,o}}{x'_{\psi,i} - x'_{\psi,o}} \tag{7}$$

For the basic elbow, $x'_{\psi,i} - x'_{\psi,o} = 0.7918$, and equation (7) becomes

$$E' = \frac{x'_{d,m} - x'_{d,o}}{0.7918} \tag{8}$$

The value of 0.7918 for $x'_{\psi,i} - x'_{\psi,o}$ is the actual entrance width for the basic elbow, whereas the approximate width as given by equations discussed in appendix B is $\pi/4$ or 0.7854. Values of $x'_{d,m} - x'_{d,o}$ as a function of K for four values of Re_0 are plotted in figure 8.

The collection efficiency of the basic elbow, obtained by equation (8) and the data of figure 8, is presented in figure 9 as a function of K for four values of Re_0 and in table I for some typical values of K and Re_0. For a given value of Re_0, the collection efficiency increases with increasing K until all the droplets entering the elbow impinge upon the outside wall. The value of K for which the collection efficiency is unity increases with increasing values of Re_0.

Rate of water interception W'_m. - The total rate of water interception is defined for the elbow as the amount of water intercepted per unit of time by a unit depth of elbow. Depth is measured in a direction perpendicular to the plane of flow (perpendicular to plane of fig. 2). The total rate of water interception is determined by the spacing of the two trajectories that define the extent of impingement $x'_{d,m} - x'_{d,o}$, the liquid-water content w, and the free-stream velocity U. For the basic elbow the total rate of water interception can be calculated from the information in figure 8 and the following relation:

$$W'_m = 0.33(x'_{d,m} - x'_{d,o})lUw \tag{9}$$

where U is in miles per hour and w is in grams per cubic meter. The total rate of water interception can also be determined from the collection efficiency E' (fig. 8) and the following relation:

$$W'_m = 0.33E'(x'_{\psi,i} - x'_{\psi,o})lUw \tag{10}$$

where $x'_{\psi,i} - x'_{\psi,o}$ is the width of the elbow entrance. Since $x'_{\psi,i} - x'_{\psi,o} = 0.7918$ for the basic elbow, equation (10) reduces to

$$W'_m = 0.261E'lUw \tag{11}$$

The linear parameter l appears in equations (9), (10), and (11) in order that W'_m have dimensions, and the depth in these equations is measured in feet.

Local rate of droplet impingement W'_β. - A knowledge of the local rate of droplet impingement is required in the design of certain types of thermal anti-icing systems. This rate, which is defined as the amount of water impinging per unit time per unit area of elbow surface, can be determined by the following expression:

$$W'_\beta = 0.33Uw\frac{dx'_d}{dS'} = 0.33Uw\beta' \tag{12}$$

(U is in mph). The quantity $0.33Uw$ of equation (12) is the amount of water entering the elbow per unit time per unit area, and the local impingement efficiency dx'_d/dS or β' is proportional to the ratio of a unit area at the entrance to the area of impingement on the wall of the droplets that enter through the unit area at the elbow entrance. The values of β' as function of S' for various combinations of K and Re_0 are presented in figure 10. The values of β' were obtained by graphically determining the reciprocals of the slopes of the curves

presented in figure 6. The curves of figure 10 show that the maximum value of β', and therefore the maximum local rate of droplet impingement W_β, occurs between $S' = 3$ and $S' = 5$ for all combinations of values of K and Re_0 studied.

The dashed lines in figure 10 are the limits in S of the impingement area, and β' is zero for any combination of K, Re_0, and S that falls beyond this limit. For some combinations of K and Re_0 (e.g., $K = 1$, $Re_0 = 128$, fig. 10(c)), the β' curves do not meet this limit within the elbow ($S = 6.46$). In these cases, impingement occurs throughout the entire length of the elbow and may extend into a straight duct attached to the exit. The value of β' and the maximum extent of impingement in the straight duct can be estimated by extrapolating the curves of figure 10 beyond $S = 6.46$ until $\beta' = 0$. The largest value that β' may have at the exit of the elbow for any combination of values of K and Re_0 is determined by the dashed line and is approximately 0.08. Thus, for any point beyond the exit on the wall of a straight duct, the values of β' will be less than 0.08.

Supplementary Elbows

In some applications, supplementary elbows, which may be derived from the flow field of the basic elbow by selecting any pair of streamlines as walls, may be more desirable than the basic elbow. Therefore, droplet impingement data for them are desirable and may be determined from the series of droplet trajectories calculated for the various combinations of K and Re_0 for the basic elbow. However, the presentation of the impingement characteristics for all possible supplementary elbows in the same manner as for the basic elbows is impractical because of the limitless number of elbows possible. During analysis of the impingement data for supplementary elbows, it was discovered that certain relations were valid along lines of constant S, so that all the important characteristics required to calculate the extent, the rate, and the distribution of impingement could be determined for any supplementary elbow from those for the basic elbow by equations that contain empirically determined coefficients. In these equations, $x_{\psi,o}$, which is determined by the streamline chosen for the outside wall, is an independent variable. A supplementary elbow may be formed from the basic elbow by choosing other streamlines for either the outside wall or the inside wall or both. The empirical equations are, however, either independent of the inside wall $x_{\psi,i}$ or depend on it only in the form $x_{\psi,i} - x_{\psi,o}$, the entrance width. The value of $x_{\psi,i}$ does, nevertheless, establish a limit to the range within which the equations are valid for the elbow chosen.

Maximum extent of impingement S_m. - Curves of S as a function of x_d, similar to those of figure 6 for the basic elbow, can be obtained for any supplementary elbow by the following empirical equation:

$$(x_d)_S = \alpha\,(x_{\psi,o} - 0.0218) + (x_d')_S \qquad (13)$$

where

$(x_d)_S$ abscissa of droplet at elbow entrance impinging on outside wall of supplementary elbow at distance S from entrance

$(\ )_S$ denotes that value for S for x_d is same as that for x_d'

α empirical coefficient, function of S, K, and Re_0 (fig. 11)

$x_{\psi,o}$ abscissa at elbow entrance of streamline designated as outside wall

0.0218 constant, abscissa at entrance of outside wall of basic elbow

$(x_d')_S$ abscissa at elbow entrance of droplet impinging on outside wall of basic elbow at distance S from entrance (fig. 6)

The values of K and Re_0 that apply to $(x_d)_S$ are the same as those for $(x_d')_S$. For some combinations of S, K, and Re_0, equation (13) will give values of x_d larger than $x_{\psi,i}$, the inside wall of the supplementary elbow. In this case, all the droplets that enter the elbow impinge upon the outside wall. As an example of the use of equation (13), assume that it is desired to find x_d of a droplet that impinges at $S = 3.0$ on the streamline $\psi = \pi 7U/4$ ($x_{\psi,o} = 0.4191$ from table II and eq. (6)), designated as outside wall for $K = 1$ and $Re_0 = 32$. From figure 6(b) at $S = 3.0$, $x_d' = 0.142$ and from figure 11(b) $\alpha = 1.502$. Substitution of these values into equation (13) gives

$$(x_d)_{3.0} = 1.502\,(0.4191 - 0.0218) + 0.142 = 0.739$$

Curves of S as a function of x_d for a supplementary elbow, similar to those of figure 6 for the basic elbow, are obtained from equation (13). The range over which values of S may be selected depends upon the particular streamline designated as the outside wall of the supplementary elbow (see fig. 2). The range of S as a function of $x_{\psi,o}$ is presented in figure 12. After the curves of S as a function of x_d are established for a particular supplementary elbow, the maximum extent of impingement S_m is found in the same manner as for the basic elbow.

Collection efficiency E. - The collection efficiency for any supplementary elbow can be calculated from the curves of S as a function of x_d (as determined in the preceding section) by the following equation:

$$E = \frac{x_{d,m} - x_{d,o}}{x_{\psi,i} - x_{\psi,o}} \tag{14}$$

which is similar to equation (7) for the basic elbow. However, an analysis of the impingement data for the supplementary elbows showed that the collection efficiency for any supplementary elbow could be determined from the collection efficiency E' for the basic elbow by the following empirical equation:

$$E = \frac{E'(x'_{\psi,i} - x'_{\psi,o}) + \gamma(x_{\psi,o} - x'_{\psi,o})}{x_{\psi,i} - x_{\psi,o}} \tag{15}$$

where

E' collection efficiency of basic elbow for given combination of K and Re_0

$x'_{\psi,i} - x'_{\psi,o}$ entrance width of basic elbow, equal to 0.7918

γ empirical coefficient, function of K and Re_0 (fig. 13)

$x_{\psi,o} - x'_{\psi,o}$ difference in abscissa of outside walls of supplementary and basic elbow

$x'_{\psi,o}$ 0.0218

$x_{\psi,i} - x_{\psi,o}$ entrance width of supplementary elbow

Substitution of the appropriate values for the basic elbow in equation (15) gives

$$E = \frac{0.7918E' + \gamma(x_{\psi,o} - 0.0218)}{x_{\psi,i} - x_{\psi,o}} \tag{16}$$

As an example of the use of equation (16), assume that the collection efficiency for a supplementary elbow defined by $x_{\psi,o} = 0.2$ and $x_{\psi,i} = 0.8$ is desired for $K = 1$ and $Re_0 = 128$. From figure 9, $E' = 0.484$ for the basic elbow, and from figure 13, $\gamma = 0.715$. Substitution of these values in equation (16) gives

$$E = \frac{0.7918(0.484) + 0.715(0.2 - 0.0218)}{0.6} = 0.851$$

In some cases the collection efficiency as given by equation (16) will be greater than unity. In this case, all the droplets that enter the elbow impinge upon the outside wall ahead of the exit, and the collection efficiency is assumed to be unity.

Rate of water interception W_m. - The total rate of water interception per unit depth for a supplementary elbow can be obtained from the following equation, which is identical in form to equation (10) for the basic elbow:

$$W_m = 0.33E(x_{\psi,i} - x_{\psi,o})lUw \tag{17}$$

in which

E	collection efficiency for supplementary elbow (determined by eq. (16))
$x_{\psi,i} - x_{\psi,o}$	entrance width
U	free-stream velocity, mph
w	liquid-water content, g/cu m

Local rate of droplet impingement W_β. - The local rate of droplet impingement for a supplementary elbow can be determined by

$$W_\beta = 0.33Uw\frac{dx_d}{dS} = 0.33Uw\beta \tag{18}$$

which is identical in form to equation (12) for the basic elbow. The values of the local impingement efficiency β as a function of S may be determined by two methods. The first method is identical to the procedure for the basic elbow. Curves of S as a function of x_d are established by equation (13) for a particular supplementary elbow and values of K and Re_0. The reciprocal of the slopes of these curves is equal to β. The second method is based upon the definition of the local impingement efficiency

$$\beta = \frac{dx_d}{dS} \tag{19}$$

and equation (13):

$$(x_d)_S = \alpha(x_{\psi,o} - 0.0218) + (x_d')_S \tag{13}$$

Differentiating equation (13) with respect to S gives

$$\beta = \frac{d(x_d)_S}{dS} = \frac{d\alpha}{dS}(x_{\psi,o} - 0.0218) + \frac{d(x_d')_S}{dS} \tag{20}$$

where

$\frac{d\alpha}{dS}$ derivative of α curves (fig. 11)

$x_{\psi,o}$ abscissa of outside wall of supplementary elbow at entrance

$\frac{d(x_d')_S}{dS}$ equal to β' for basic elbow at given value of S (fig. 10)

and equation (20) may be written

$$\beta = \frac{d\alpha}{dS}(x_{\psi,o} - 0.0218) + \beta' \tag{21}$$

Values of $d\alpha/dS$ as a function of S for various values of K and Re_o are presented in figure 14. These values were determined graphically from the data of figure 11.

The values of K and Re_o that apply to β are the same as those for β'. As an example of the use of equation (21), assume that β is required at $S = 3.0$ for a supplementary elbow, the outside wall of which is defined by $x_{\psi,o} = 0.2$, and K and Re_o are equal to 1 and 32, respectively. From figure 14(b), $d\alpha/dS = 0.345$ at $S = 3.0$, and from figure 10(b), $\beta' = 0.152$ so that

$$\beta = 0.345(0.2 - 0.0218) + 0.152 = 0.213$$

Some caution must be exercised in using equation (18), because values of the local rate of impingement may be calculated for a supplementary elbow that are correct but may or may not actually exist, depending upon which streamline is selected as the inside wall of the elbow. The inside wall for some values of K and Re_o determines the maximum extent of impingement S_m. Therefore equation (18) should be used in conjunction with the maximum extent of impingement S_m when calculating

β or W_β for a particular supplementary elbow; β and W_β are both zero for distances greater than S_m.

IMPINGEMENT IN CLOUDS OF NONUNIFORM DROPLET SIZE

The impingement data and equations presented in the preceding sections, by which the extent, the rate, and the distribution of droplet impingement can be determined for the basic and supplementary elbows, apply directly to clouds composed of droplets of uniform size. Clouds, however, are not necessarily composed of droplets of uniform size but may have a large range of droplet size. For clouds composed of droplets of nonuniform size, the maximum extent of impingement for elbows is determined by the smallest droplet size present in the cloud. (This is in contrast to the situation involving external aerodynamics or flow around a wing or other body, where the largest droplet determines the maximum extent of impingement.) In order to determine the total and local rates of droplet impingement by equations (10) or (17) and (12) or (18), respectively, for clouds composed of droplets of nonuniform size, the collection efficiency and the local impingement efficiency must be modified. These modified values can be obtained for a given droplet-size distribution pattern by weighting the values of these two quantities for a given size according to the amount of liquid water contained in the given droplet size. A detailed procedure for determining a weighted collection efficiency for a given droplet-size distribution pattern is presented in reference 4. A similar procedure can be used to determine a weighted local impingement efficiency.

CONCLUDING REMARKS

The special 90° elbows for which droplet impingement data are presented in this report are suitable for use in aircraft air-intake ducts and as droplet inertia separators. For droplet inertia separators, it may be necessary to combine two or more elbows so as to produce a turn of 180° or more in order to obtain satisfactory separation of droplets from the air. The impingement data for supplementary elbows defined by streamlines near the inside wall of the basic elbow can probably be used to approximate droplet impingement in conventional elbows with long radii of curvature, because streamlines in this region are approximately equidistant apart at all points throughout the elbow (see figs. 2 and 4 and table II).

The maximum extent of impingement for these elbows varies directly with the free-stream Reynolds number and inversely with inertia parameter. In contrast to airfoils, the maximum extent of impingement varies inversely with droplet size. For a given value of free-stream Reynolds

number, the collection efficiency for the basic elbow increases with increasing values of inertia parameter until all droplets that enter the elbow impinge upon the outside wall. The value of inertia parameter for which the collection efficiency becomes unity increases with increasing values of free-stream Reynolds number. The length of the outside wall of the basic elbow is 6.46 S units (distance from entrance), and the maximum local rate of droplet impingement occurs between $S = 3$ and $S = 5$ for all investigated combinations of free-stream Reynolds number and inertia parameter.

The use of elbows and bends designed according to potential theory for aircraft ducts and inlets has two advantages: The pressure losses are much less than those for conventional elbows or any arbitrary bend; and droplet trajectories with respect to the elbow are obtainable, since the air-flow field is easily established by potential theory. Elbows designed for potential flow need not be restricted to symmetrical 90° bends, for potential functions exist by which elbows with various sizes, odd shapes and angles of bend, and different entrance and exit cross-sectional areas can be designed.

Lewis Flight Propulsion Laboratory
National Advisory Committee for Aeronautics
Cleveland, Ohio, July 9, 1953

W_m rate of water impingement on total elbow surface per unit depth of elbow, lb/(hr)(ft of depth)

W_β local rate of water impingement on elbow surface, lb/(hr)(sq ft)

w liquid-water content of cloud, g/cu m

x,y rectangular coordinates, ratio to l, dimensionless

x_d abscissa at elbow entrance of any droplet trajectory, dimensionless

$x_{d,m}$ maximum value of abscissa at elbow entrance of droplet trajectory that intersects or is tangent to streamline designated as outside wall of elbow, dimensionless

$x_{d,o}$ minimum value of abscissa at elbow entrance of droplet trajectory (has same value as $x_{\psi,o}$), dimensionless

x_ψ abscissa at elbow entrance of any air streamline inside elbow, dimensionless

$x_{\psi,i}$ abscissa at elbow entrance of streamline designated as inside wall, dimensionless

$x_{\psi,o}$ abscissa at elbow entrance of streamline designated as outside wall, dimensionless

α empirical coefficient, dimensionless

β local impingement efficiency, dimensionless

γ empirical coefficient, dimensionless

ζ complex number, $\zeta = \xi + i\eta$

θ angle made by wall of elbow and plane of flow field

μ viscosity of air, slugs/(ft)(sec)

ξ,η rectangular coordinates, ft

ρ density, slugs/cu ft

τ time parameter tU/l, dimensionless

φ velocity potential

APPENDIX A

SYMBOLS

The following symbols are used in this report:

a	droplet radius, ft
C_D	drag coefficient for droplets, dimensionless
d	droplet diameter, microns (3.28×10^{-6} ft)
E	collection efficiency, ratio of amount of water impinging within elbow to amount of water entering elbow, dimensionless
i	imaginary number, $\sqrt{-1}$
K	inertia parameter, $\frac{2}{9}\frac{\rho_w a^2 U}{\mu l}$, where U is in ft/sec, dimensionless
L	width of basic elbow at entrance, $\pi l/4$, ft
l	arbitrary length, proportional to size of elbow, ft
Re	local Reynolds number with respect to droplet, $2a\rho_a\bar{v}/\mu$, dimensionless
Re_0	free-stream Reynolds number with respect to droplet, $2a\rho_a U/\mu$
S	distance along outside wall of elbow, measured from entrance, ratio to l, dimensionless
S_m	maximum extent of impingement
t	time, sec
U	free-stream or entrance velocity, mph or ft/sec as noted
u	local air velocity, ratio to U, dimensionless
v	local droplet velocity, ratio to U, dimensionless
$\bar{v}$	magnitude of local vector difference between droplet and air velocity, ft/sec

ψ stream function

ω complex potential, $\omega = \varphi + i\psi$

Subscripts:

a air

S constant distance from elbow entrance

w water

x horizontal component

y vertical component

η vertical component

ξ horizontal component

Superscript:

' refers to basic elbow defined by streamlines $\psi = \pi lU/8$ and $3\pi lU/8$

APPENDIX B

SELECTION OF COMPLEX POTENTIAL FUNCTION FOR DESIGN OF 90° ELBOW AND CALCULATION OF FLOW FIELD

The 90° elbows for which droplet impingement data are presented in the body of the report were designed by selecting as walls of an elbow two streamlines of a two-dimensional incompressible flow field established by a complex potential function. This function, which nearly satisfies all the criteria outlined in the ANALYSIS for a 90° elbow, is discussed in references 13 and 14. It can be expressed in the following form:

$$e^{(i+1)\zeta/l} = e^{(i+1)\omega/lU} + e^{(i-1)\omega/lU} \tag{5}$$

where

i $\sqrt{-1}$

ζ $\xi + i\eta$

l linear parameter proportional to size of elbow

ω $\varphi + i\psi$

U constant, velocity of uniform stream at infinity before and after bend

φ velocity potential

ψ stream function

Calculation of Streamlines

Parametric equations for the flow streamlines are obtained from equation (5) by separating and equating the real and imaginary parts of the ζ function to the real and imaginary parts of the ω function. The results of this procedure are:

$$\xi = \frac{l}{2} \arctan\left(\frac{\cot\frac{\psi}{lU} + \cot\frac{\varphi}{lU}\tanh\frac{\varphi}{lU}}{\cot\frac{\varphi}{lU}\cot\frac{\psi}{lU} - \tanh\frac{\varphi}{lU}}\right) + \frac{l}{2}\left[-\frac{\psi}{lU} + \ln\sqrt{2\left(\cosh 2\frac{\varphi}{lU} + \cos 2\frac{\psi}{lU}\right)}\right] \tag{B1}$$

and

$$\eta = \frac{l}{2} \arctan\left(\frac{\cot\frac{\psi}{lU} + \cot\frac{\varphi}{lU}\tanh\frac{\varphi}{lU}}{\cot\frac{\varphi}{lU}\cot\frac{\psi}{lU} - \tanh\frac{\varphi}{lU}}\right) - \frac{l}{2}\left[-\frac{\psi}{lU} + \ln\sqrt{2\left(\cosh 2\frac{\varphi}{lU} + \cos 2\frac{\psi}{lU}\right)}\right] \tag{B2}$$

When mapping a streamline (ψ = constant) in the ξ,η-plane by equations (B1) and (B2), the velocity potential φ is considered as a variable parameter. A portion of the streamline pattern given by equations (B1) and (B2) is presented in figure 1.

Velocity Calculations

Parametric equations for determining the velocity components of the flow field are obtained by differentiating equation (5) with respect to ζ and separating the real and imaginary parts. The real part is equal to the ξ-component of velocity and the imaginary part is the η-component of velocity. The results of this procedure are

$$u_\xi = U\frac{\sinh\frac{2\varphi}{lU} + \sin\frac{2\psi}{lU} + \cos\frac{2\psi}{lU} + \cosh\frac{2\varphi}{lU}}{2\cosh\frac{2\varphi}{lU} + 2\sin\frac{2\psi}{lU}} \tag{B3}$$

and

$$u_\eta = U\frac{\cos\frac{2\psi}{lU} + \sin\frac{2\psi}{lU} + \cosh\frac{2\varphi}{lU} - \sinh\frac{2\varphi}{lU}}{2\cosh\frac{2\varphi}{lU} + 2\sin\frac{2\psi}{lU}} \tag{B4}$$

When the velocity components are determined along a streamline (ψ = constant) by equations (B3) and (B4), the velocity potential φ is considered as a variable parameter. The resultant local velocity u at a point in the flow field is given by

$$u = \sqrt{u_\xi^2 + u_\eta^2} = U\sqrt{\frac{\cosh 2\frac{\varphi}{lU} + \cos 2\frac{\psi}{lU}}{\cosh 2\frac{\varphi}{lU} + \sin 2\frac{\psi}{lU}}} \qquad \text{(B5)}$$

Walls and Ends of Elbow

It can be shown (ref. 13) that the flow between the two streamlines $\psi = \pi lU/8$ and $3\pi lU/8$ (indicated by heavy lines in fig. 1) satisfies all the criteria for an elbow outlined in the body of the report. Therefore, these two streamlines were selected as walls of the basic elbow for this study.

The first criterion is strictly fulfilled only at infinity, as the stream before and after the bend rapidly approaches uniform and rectilinear motion asymptotically. Therefore, the ends of the elbow may be selected at some reasonable distance before and after the bend without serious error. For this droplet impingement study, $\xi = 3\pi l/4$ and $\eta = -3\pi l/4$ (indicated by dashed lines in fig. 1) were selected as the ends of the elbow. At the intersection of $\xi = 3\pi l/4$ and the streamline $\psi = \pi lU/8$, the ξ and η components of velocity u_ξ and u_η are equal to 0.9999U and 0.01280U, respectively, where U is the velocity of the stream at infinity (free-stream velocity). At the intersection of $\xi = 3\pi l/4$ and the streamline $\psi = 3\pi lU/8$, the velocity components u_ξ and u_η are equal to 0.98738U and 0.00008U, respectively. Since the flow is symmetric with respect to the bisector of the angle of bend (line AO, fig. 1), the velocity components at the corresponding points at the other end of the elbow are identical, except that the ξ and η components are reversed. The error in assuming that the flow between streamlines $\psi = \pi lU/8$ and $3\pi lU/8$ is uniform and rectilinear with free-stream velocity U at $\xi = 3\pi l/4$ and $\eta = -3\pi l/4$ is approximately 1 percent.

Since the flow between the streamlines $\psi = \pi lU/8$ and $3\pi lU/8$ satisfies the assumed criteria for the design of an elbow, any pair of streamlines between these two streamlines may also be selected as the walls of an elbow. However, an elbow defined by the two basic streamlines is probably the most practical elbow with respect to width of entrance and turning radius, as will be discussed in the next section.

Relation Between l and Elbow Size

The linear parameter l of the complex potential function (eq. (5)) is related to the size of the elbow through two quantities: the width of the entrance and a quantity that may be regarded as the turning radius of the elbow. The relations between the coordinates and the stream function ψ at infinity are

$$\eta = \frac{\psi}{U} \quad \text{for} \quad \xi = \infty \tag{B6}$$

and

$$\xi = -\frac{\psi}{U} \quad \text{for} \quad \eta = \infty \tag{B7}$$

From which the spacing of streamlines (width of elbow) can be determined at infinity. For example, for the basic elbow defined by $\psi = \pi lU/8$ and $3\pi lU/8$, the width of the elbow at $\eta = -\infty$ is $\pi l/4$. The error in elbow entrance width caused by terminating the basic elbow at $\xi = 3\pi l/4$ and $\eta = -3\pi l/4$ (fig. 1) and assuming that the elbow entrance width is $\pi l/4$ is less than 1 percent, because the streamlines between these points and infinity are almost parallel to each other and to the coordinate axis. Since this error is small, equations (B6) and (B7) can be used to find the approximate width of the basic elbow and all supplementary elbows defined by other pairs of streamlines.

The point A $\left(\frac{3\pi l}{4}, -\frac{3\pi l}{4}\right)$ in figure 1 may be regarded as the center of turning of the basic elbow or any supplementary elbow. A radius of turning of an elbow wall or any streamline may be defined as the distance from point A, measured along the lines defined by the ends of the elbow, to the elbow wall or the streamline. The radius of turning for a particular wall or streamline is porportional to l and is determined by adding $3\pi l/4$ to the distance between the wall or streamline and the ξ- or η-axis. This distance can be approximated by equations (B6) or (B7). For example, for the basic elbow, the average radius of turning may be defined as the distance from point A (fig. 1) to the midpoint of the entrance, point B. The streamline $\psi = \pi lU/4$ defines the midpoint of the entrance. The distance between this point and the η-axis is approximately $\pi l/4$ (from eq. (B7)), and the average radius of turning for the basic elbow is approximately

$$\frac{3\pi l}{4} + \frac{\pi l}{4} = \pi l \tag{B8}$$

Inasmuch as the width of an elbow at the entrance and the radius of turning are both proportional to l, the basic elbow is probably the most practical elbow, because for a given entrance width (physical units such as ft) the turning radius is smaller for this elbow than for any elbow defined by a pair of streamlines between $\psi = \pi lU/8$ and $.3\pi lU/8$.

Elbow Cross Sections

An elbow with any entrance cross-section configuration that satisfies all the criteria outlined in the body of this report may be designed by the use of equations (B1) and (B2). The only conditions to be satisfied are that those streamlines forming the walls of the elbow at the entrance must remain on the walls throughout the elbow and must be identical to or intermediate to those defining the basic elbow. For an elbow with a rectangular entrance cross section, the cross sections at all points along the elbow are rectangular. However, the width of the elbow changes while the depth remains constant. For an elbow with a circular entrance cross section, the cross sections change to egg-shaped in the center of the elbow. The depth, however, remains constant throughout the elbow. Some typical cross sections are presented in figure 4 for a rectangular and a circular elbow entrance. The walls for the rectangular elbow and the circular elbow at the maximum diameter are defined by the streamlines $\psi = \pi lU/8$ and $3\pi lU/8$ (basic elbow walls). The cross sections presented in figure 4 are normal cross sections, that is, perpendicular to the streamlines, or along constant velocity potential surfaces (φ = constant in eqs. (B1) and (B2)).

Elbow and Flow Field in Dimensionless Form

For droplet impingement studies for airfoils and other aircraft components, it is convenient to express the results in terms of dimensionless parameters, so that the results may apply to a wide range of flight and meteorological conditions as well as a wide range of size of airfoils and components (refs. 2 and 4). In order to obtain the impingement results in terms of dimensionless parameters by analog computer technique, the aircraft component and the flow field must be expressed in terms of dimensionless parameters. This necessity is met for airfoils by expressing all distances as ratios to chord length and all velocities as ratios to free-stream velocity. The elbow and its velocity field can be expressed in dimensionless form by expressing distances as ratios to the arbitrary length l and velocities as ratios to the free-stream velocity U; thus, for the elbow walls and intermediate streamlines, both sides of equations (B1) and (B2) are divided by l, and for the flow field, both sides of equations (B3) and (B4) are divided by the free-stream velocity U.

The basic elbow and some typical streamlines are presented in terms of dimensionless coordinates in graphical form in figure 2 and in tabular form in table II. In figure 2 the origin of the coordinate system was so translated that the elbow is entirely in the first quadrant. The translation of the origin was made in order to facilitate trajectory calculation by the mechanical analog computer. The relations between x and y of figure 2 and ξ and η of figure 1 are

$$\left.\begin{aligned} x &= \frac{\xi}{l} + 1.2 \\ \text{and} \qquad y &= \frac{\eta}{l} + 2.4 \end{aligned}\right\} \tag{6}$$

The velocity field for the basic elbow is presented in figure 3. Figure 3(a) gives the x-component of velocity u_x as a function of x for constant values of y, and figure 3(b) gives the y-component of velocity u_y as a function of y for constant values of x. The component velocities u_x and u_y are dimensionless and are equal to u_ξ/U and u_η/U, respectively. A comparison of figures 3(a) and (b) shows that the velocity field is symmetrical with respect to the bisector of the angle of bend of the elbow, since for comparable points before and after the bend the x- and y-components are identical except for being interchanged.

The coordinates, the velocity components, and the distance from entrance of points along a streamline are given in table II in dimensionless form as functions of φ/lU, the variable parameter of equations (B1) to (B4).

APPENDIX C

METHOD OF DETERMINING IMPINGEMENT CHARACTERISTICS OF ELBOWS WITH NONRECTANGULAR ENTRANCE CROSS SECTIONS

The impingement in elbows with nonrectangular entrance cross sections can be determined approximately from the results presented in the body of the report for rectangular elbows. The nonrectangular elbow section can be approximated by a series of rectangular elbows, as shown by the dashed lines in figure 4(b). The accuracy with which the impingement characteristics can be determined depends upon the number of small rectangular elbows used to approximate the nonrectangular cross section.

The extent of impingement, the collection efficiency, the total rate of water interception, and the local rate of droplet impingement can be determined for each of the small rectangular elbows from the results for the basic and supplementary elbows. The impingement characteristics of the entire elbow are obtained from those for the individual small rectangular elbows in the following manner:

Extent of Impingement

A curve representing the maximum extent of impingement on the wall of a nonrectangular elbow can be plotted by spotting points, which represent the maximum extent of impingement for each small rectangular elbow, on the wall of the elbow.

Collection Efficiency

The collection efficiency for a nonrectangular elbow can be determined by the following expression:

$$E = \sum_{j=1}^{j=n} \frac{A_j}{A} E_j$$

where

n number of small rectangular elbows into which large nonrectangular elbow is divided

A_j area at entrance of each small rectangular elbow

A area of entrance cross section of nonrectangular elbow

E_j collection efficiency of each small rectangular elbow

2847

The collection efficiency E_j for each small rectangular elbow is obtained from results for the basic and supplementary elbows.

Total Rate of Water Interception

The total rate of water interception for a nonrectangular elbow is the sum of the total rates of water interception for the small rectangular elbows. The rates of water interception for the small rectangular elbows can be found by equations (11) or (17) or both. Equations (11) and (17) give the rate of water interception per unit depth for rectangular elbows. Therefore, for each small rectangular elbow the quantity given by equations (11) and (17) must be multiplied by the depth of small rectangular elbow in feet before the summation is made to find the total rate of water interception for the nonrectangular elbow.

Local Rate of Droplet Impingement

The local rate of droplet impingement for elbows with nonrectangular entrances can be determined by equations (12) or (18) or both for basic and supplementary elbows by replacing β' and β with $\beta' \sin\theta$ and $\beta \sin\theta$, respectively. The local impingement efficiency β' or β was determined for elbow walls that are perpendicular to the plane of the flow field. For elbows with nonrectangular entrances, the walls are not necessarily perpendicular to the plane of the flow field but may make an angle θ (fig. 4). Therefore, when calculating the local rate of droplet impingement for an elbow with a nonrectangular entrance, the factor $\sin\theta$ accounts for the fact that the area of impingement for droplets entering the elbow through a unit area is increased when the wall makes an angle with the plane of the flow field. The angle θ is the angle between the plane of the flow field and a line tangent to the elbow surface and perpendicular to the air streamline at the point on the wall where the local rate of droplet impingement is being determined. This angle can be determined graphically from elbow cross sections as shown in figure 4(b) for point A for cross section E-F. The cross sections (fig. 4), except those for the entrance, are along surfaces perpendicular to the air streamlines, that is, along surfaces where the velocity potential φ of equations (B1) and (B2) is constant. In figure 4(b), section E-F, line AB is parallel to the plane of the flow field, line AC is tangent to the elbow wall at point A, and θ is the angle between lines AB and AC. Inasmuch as the local impingement factor β of equations (12) and (18) is given in figure 10 as a function of S and the angle θ

is determined on surfaces of constant velocity potential φ, relations between φ and S for various streamlines are required in order to determine the local rate of droplet impingement at a particular point on the wall of a nonrectangular elbow. These relations can be established from the data presented in table II.

REFERENCES

1. Brun, Rinaldo J., Serafini, John S., and Moshos, George J.: Impingement of Water Droplets on an NACA 65_1-212 Airfoil at an Angle of Attack of 4°. NACA RM E52B12, 1952.

2. Brun, Rinaldo J., Gallagher, Helen M., and Vogt, Dorothea E.: Impingement of Water Droplets on NACA 65_1-208 and 65_1-212 Airfoils at 4° Angle of Attack. NACA TN 2952, 1953.

3. Dorsch, Robert G., and Brun, Rinaldo, J.: A Method for Determining Cloud-Droplet Impingement on Swept Wings. NACA TN 2931, 1953.

4. Brun, Rinaldo J., and Mergler, Harry W.: Impingement of Water Droplets on a Cylinder in an Incompressible Flow Field and Evaluation of Rotating Multicylinder Method for Measurement of Droplet-Size Distribution, Volume-Median Droplet Size, and Liquid-Water Content in Clouds. NACA TN 2904, 1953.

5. Brun, Rinaldo J., Serafini, John S., and Gallagher, Helen M.: Impingement of Cloud Droplets on Aerodynamic Bodies as Affected by the Compressibility of Air Flow Around the Body. NACA TN 2903, 1953.

6. Glauret, Muriel: A Method of Constructing the Paths of Raindrops of Different Diameters Moving in the Neighborhood of (1) a Circular Cylinder, (2) an Aerofoil, Placed in a Uniform Stream of Air; and a Determination of the Rate of Deposit of Drops on the Surface and the Percentage of Drops Caught. R. & M. No. 2025, British, A.R.C., 1940.

7. Langmuir, Irving, and Blodgett, Katherine B.: A Mathematical Investigation of Water Droplet Trajectories. Tech. Rep. No. 5418, Air Materiel Command, AAF, Feb. 19, 1946. (Contract No. W-33-038-ac-9151 with General Electric Co.)

8. Ranz, W. E.: The Impaction of Aersol Particles on Cylindrical and Spherical Collectors. Tech. Rep. No. 3, Eng. Exp. Station, Univ. Ill., March 31, 1951. (Contract No. AT(30-3)-28, U. S. Atomic Energy Comm.)

9. Brun, Edmond, Caron, Robert, et Vasseur, Marcel: Introduction à l'étude de la Mécanique des Suspensions. G.R.A. Rapport Tech. No. 15, Recherches Aéronautiques (Paris), 1945.

10. Bergrun, Norman R.: A Method for Numerically Calculating the Area and Distribution of Water Impingement on the Leading Edge of an Airfoil in a Cloud. NACA TN 1397, 1947.

11. Guibert, A. G., Janssen, E., and Robbins, W. M.: Determination of Rate, Area, and Distribution of Impingement of Waterdrops on Various Airfoils from Trajectories Obtained on the Differential Analyzer. NACA RM 9A05, 1949.

12. Lewis, James P.: Investigation of Aerodynamic and Icing Characteristics of a Flush Alternate-Inlet Induction-System Air Scoop. NACA RM E53E07, 1953.

13. Szczeniowski, Boleslaw: Design of Elbows in Potential Motion. Jour. Aero. Sci., vol. 11, no. 1, Jan. 1944, pp. 73-75.

14. Harper, John J.: Tests on Elbows of a Special Design. Jour. Aero. Sci., vol. 13, no. 11, Nov. 1946, pp. 587-592.

TABLE I. - EXAMPLES OF INERTIA PARAMETER AND FREE-STREAM REYNOLDS NUMBER IN TERMS OF WIDTH OF BASIC ELBOW, FREE-STREAM VELOCITY, AIR DENSITY, AIR VISCOSITY, AND DROPLET DIAMETER

Elbow width, L, ft	Arbitrary length parameter, l, ft	Free-stream or entrance velocity, U, mph	Pressure altitude, ft	Air density, ρ_a, $\frac{\text{slugs}}{\text{cu ft}}$	Temperature, $^{\circ}F$	Air viscosity, μ, $\frac{\text{slugs}}{(\text{ft})(\text{sec})}$	Droplet diameter, d, microns	Inertia parameter, K	Free-stream Reynolds number, Re_0	Maximum extent of impingement for basic elbow, S'_m	Collection efficiency for basic elbow, E'
0.5	0.6366	200	10×10^3	0.001756	12	34.54×10^{-8}	10	0.1549	48.9	6.46	0.09
.5	.6366	200	10	.001756	12	34.54	25	.9676	122.3	6.46	.48
.5	.6366	200	30	.000889	-39	31.43	10	.1704	27.2	6.46	.11
.5	.6366	200	30	.000889	-39	31.43	25	1.0650	68.1	6.46	.64
.5	.6366	500	10	.001756	12	34.54	10	.3872	122.3	6.46	.20
.5	.6366	500	10	.001756	12	34.54	25	2.4180	305.8	6.46	.88
.5	.6366	500	30	.000889	-39	31.43	10	.4260	68.1	6.46	.24
.5	.6366	500	30	.000889	-39	31.43	25	2.6625	170.2	5.75	1.00
1.0	1.2732	200	10	.001756	12	34.54	10	.0774	48.9	6.46	.04
1.0	1.2732	200	10	.001756	12	34.54	25	.4838	122.3	6.46	.25
1.0	1.2732	200	30	.000889	-39	31.43	10	.0852	27.2	6.46	.05
1.0	1.2732	200	30	.000889	-39	31.43	25	.5325	68.1	6.46	.30
1.0	1.2732	500	10	.001756	12	34.54	10	.1936	122.3	6.46	.10
1.0	1.2732	500	10	.001756	12	34.54	25	1.2090	305.8	6.46	.44
1.0	1.2732	500	30	.000889	-39	31.43	10	.2130	68.1	6.46	.12
1.0	1.2732	500	30	.000889	-39	31.43	25	1.3312	170.2	6.46	.57

TABLE II. - STREAMLINE COORDINATES, VELOCITY COMPONENTS, AND DISTANCE FROM ENTRANCE AS FUNCTIONS OF VELOCITY POTENTIAL

Velocity potential, φ/lU	Stream function, ψ														
	$\pi lU/8$					$5\pi lU/32$					$3\pi lU/16$				
	Streamline coordinate		Velocity component		Distance from entrance, S	Streamline coordinate		Velocity component		Distance from entrance, S	Streamline coordinate		Velocity component		Distance from entrance, S
	ξ/l	η/l	v_ξ	v_η		ξ/l	η/l	v_ξ	v_η		ξ/l	η/l	v_ξ	v_η	
Entrance	-0.38640	-2.35619	0.01280	0.99992	0	-0.48469	-2.35619	0.01250	0.99745	0	-0.58321	-2.35619	0.01173	0.99529	0
-2.2	-.38406	-2.20004	.01721	.99985	.161	-.48238	-2.19836	.01683	.99653	.162	-.58103	-2.19673	.01583	.99336	.164
-2.0	-.37983	-2.00008	.02557	.99967	.356	-.47822	-1.99758	.02497	.99477	.369	-.57708	-1.99516	.02346	.99009	.369
-1.8	-.37356	-1.80018	.03790	.99928	.567	-.47203	-1.79647	.03694	.99208	.570	-.57120	-1.79287	.03467	.98522	.574
-1.6	-.36429	-1.60040	.05599	.99843	.770	-.46284	-1.59491	.05442	.98793	.775	-.56243	-1.58955	.05100	.97797	.783
-1.4	-.35062	-1.40087	.08231	.99661	.972	-.44923	-1.39278	.07969	.98147	.982	-.54937	-1.38483	.07450	.96720	.990
-1.2	-.33060	-1.20189	.12012	.99276	1.177	-.42916	-1.19003	.11566	.97131	1.185	-.52994	-1.17829	.10780	.95125	1.205
-1.0	-.30154	-1.00404	.17336	.98486	1.378	-.39976	-.98683	.16570	.95524	1.394	-.50113	-.96959	.15385	.92782	1.414
-.8	-.25996	-.80845	.24602	.96927	1.579	-.35718	-.78388	.23306	.92992	1.603	-.45873	-.75887	.21541	.89388	1.634
-.6	-.20166	-.61722	.34066	.94019	1.784	-.29660	-.58294	.31948	.89079	1.818	-.39715	-.54738	.29397	.84597	1.857
-.4	-.12232	-.43378	.45574	.89012	1.988	-.21279	-.38757	.42334	.83281	2.029	-.30995	-.33867	.38825	.78098	2.083
-.2	-.01855	-.26302	.58286	.81257	2.193	-.10154	-.20357	.53786	.75263	2.255	-.19155	-.13958	.49300	.69787	2.322
-.1	.04293	-.18419	.64642	.76298	2.293	-.03510	-.11813	.59566	.70440	2.361	-.11988	-.04662	.54664	.65022	2.443
.1	.18419	-.04293	.76298	.64642	2.493	.11813	.03510	.70440	.59566	2.583	.04662	.11988	.65022	.54664	2.681
.2	.26302	.01855	.81257	.58266	2.597	.20357	.10154	.75263	.53786	2.689	.13958	.19155	.69787	.49300	2.800
.4	.43378	.12232	.89012	.45574	2.798	.38757	.21279	.83281	.42334	2.909	.33867	.30995	.78098	.38825	3.034
.6	.61722	.20166	.94019	.34066	3.004	.58294	.29660	.89079	.31948	3.120	.54738	.39715	.84597	.29397	3.263
.8	.80845	.25996	.96927	.24602	3.201	.78388	.35718	.92992	.23306	3.331	.75887	.45873	.89388	.21541	3.485
1.0	1.00404	.30154	.98486	.17336	3.402	.98683	.39976	.95524	.16570	3.542	.96959	.50113	.92782	.15385	3.706
1.2	1.20189	.33060	.99276	.12012	3.600	1.19003	.42916	.97131	.11566	3.751	1.17829	.52994	.95125	.10780	3.917
1.4	1.40087	.35062	.99661	.08231	3.807	1.39278	.44923	.98147	.07969	3.956	1.38483	.54937	.96720	.07450	4.126
1.6	1.60040	.36429	.99843	.05599	4.012	1.59491	.46284	.98793	.05442	4.165	1.58955	.56243	.97797	.05100	4.344
1.8	1.80018	.37356	.99928	.03790	4.217	1.79647	.47203	.99208	.03694	4.372	1.79287	.57120	.98522	.03467	4.542
2.0	2.00008	.37983	.99967	.02557	4.416	1.99758	.47822	.99477	.02497	4.571	1.99516	.57708	.99009	.02346	4.751
2.2	2.20004	.38406	.99985	.01721	4.618	2.19836	.48238	.99653	.01683	4.776	2.19673	.58103	.99336	.01583	4.956
Exit	2.35619	.38640	.99992	.01280	4.780	2.35619	.48469	.99745	.01250	4.940	2.35619	.58321	.99529	.01173	5.114
	$7\pi lU/32$					$\pi lU/4$					$9\pi lU/32$				
Entrance	-0.68196	-2.35619	0.01053	0.99294	0	-0.78089	-2.35619	0.00696	0.99104	0	-0.88002	-2.33619	0.00703	0.98951	0
-2.2	-.67999	-2.19523	.01424	.99044	.165	-.77922	-2.19390	.01213	.98787	.166	-.87870	-2.19280	.00956	.98576	.166
-2.0	-.67641	-1.99291	.02111	.98579	.373	-.77616	-1.99093	.01799	.98201	.372	-.87627	-1.98928	.01421	.97889	.376
-1.8	-.67108	-1.78951	.03118	.97893	.574	-.77155	-1.78653	.02660	.97340	.581	-.87260	-1.78404	.02107	.96882	.582
-1.6	-.66305	-1.58453	.04585	.96885	.788	-.76461	-1.58004	.03917	.96083	.792	-.86702	-1.57628	.03115	.95415	.795
-1.4	-.65102	-1.37733	.06697	.95416	.998	-.75411	-1.37056	.05732	.94268	1.003	-.85849	-1.36480	.04584	.93303	1.011
-1.2	-.63294	-1.16707	.09687	.93297	1.216	-.73811	-1.15681	.08317	.91683	1.223	-.84529	-1.14795	.06703	.90313	1.232
-1.0	-.60574	-.95287	.13823	.90291	1.427	-.71360	-.93728	.11920	.88080	1.446	-.82460	-.92348	.09709	.86177	1.458
-.8	-.56487	-.73410	.19360	.86122	1.660	-.67560	-.71038	.16798	.83202	1.682	-.79162	-.68867	.13878	.80640	1.700
-.6	-.50389	-.51124	.26457	.80532	1.892	-.61741	-.47543	.23148	.76852	1.925	-.73831	-.44115	.19468	.73543	1.958
-.4	-.41473	-.28754	.35053	.73363	2.134	-.52828	-.23483	.31003	.68997	2.187	-.65202	-.18156	.26637	.64947	2.231
-.2	-.28965	-.07093	.44770	.64692	2.392	-.39736	.00249	.40131	.59869	2.462	-.51678	.08075	.35308	.55230	2.532
-.1	-.21241	.03080	.49844	.59906	2.521	-.31412	.11478	.45017	.54983	2.603	-.42703	.20617	.40094	.50156	2.692
.1	-.03080	.21241	.59906	.49844	2.781	-.11478	.31412	.54983	.45017	2.890	-.20617	.42703	.50156	.40094	3.014
.2	..07093	.28965	.64692	.44770	2.912	-.00249	.39736	.59869	.40131	3.032	-.08075	.51678	.55230	.35308	3.161
.4	.28754	.41473	.73363	.35053	3.160	.23483	.52828	.68997	.31003	3.306	.18156	.65202	.64947	.26637	3.463
.6	.51124	.50389	.80532	.26457	3.408	.47543	.61741	.76852	.23148	3.570	.44115	.73831	.73543	.19468	3.742
.8	.73410	.56487	.86122	.19360	3.645	.71038	.67560	.83202	.16798	3.808	.68867	.79162	.80640	.13878	4.003
1.0	.95287	.60574	.90291	.13823	3.869	.93728	.71360	.88080	.11920	4.046	.92348	.82460	.86177	.09709	4.243
1.2	1.16707	.63294	.93297	.09687	4.087	1.15681	.73811	.91683	.08317	4.267	1.14795	.84529	.90313	.06703	4.429
1.4	1.37733	.65102	.95416	.06697	4.296	1.37056	.75411	.94268	.05732	4.484	1.36480	.85849	.93303	.04584	4.688
1.6	1.58453	.66305	.96885	.04585	4.508	1.58004	.76461	.96083	.03917	4.698	1.57628	.86702	.95415	.03115	4.905
1.8	1.78951	.67106	.97893	.03118	4.722	1.78653	.77155	.97340	.02660	4.913	1.78404	.87260	.96882	.02107	5.115
2.0	1.99291	.67641	.98579	.02111	4.924	1.99093	.77616	.98201	.01799	5.116	1.98928	.87627	.97889	.01421	5.323
2.2	2.19523	.67999	.99044	.01424	5.131	2.19390	.77922	.98787	.01213	5.321	2.19280	.87870	.98576	.00956	5.528
Exit	2.35619	.68196	.99294	.01053	5.294	2.35619	.78089	.99104	.00896	5.484	2.35619	.88002	.98951	.00703	5.694
	$5\pi lU/16$					$11\pi lU/32$					$3\pi lU/8$				
Entrance	-0.97846	-2.35619	0.00568	0.98836	0	-1.07870	-2.35619	0.00252	0.98764	0	-1.17815	-2.35619	0.00008	0.98738	0
-2.2	-.97837	-2.19198	.00664	.98417	.165	-1.07818	-2.19147	.00347	.98317	.164	-1.17806	-2.19128	.00015	.98279	.165
-2.0	-.97667	-1.98804	.00991	.97654	.376	-1.07728	-1.98725	.00523	.97503	.376	-1.17801	-1.98696	.00033	.97443	.376
-1.8	-.97409	-1.78215	.01478	.96533	.582	-1.07591	-1.78095	.00792	.96306	.580	-1.17791	-1.78099	.00072	.96210	.584
-1.6	-.97012	-1.57359	.02203	.94900	.799	-1.07374	-1.57151	.01207	.94558	.796	-1.17767	-1.57076	.00157	.94401	.800
-1.4	-.96397	-1.36033	.03280	.92550	1.016	-1.07028	-1.35736	.01853	.92031	1.014	-1.17712	-1.35608	.00339	.91769	1.014
-1.2	-.95423	-1.14091	.04875	.89220	1.235	-1.06457	-1.13608	.02869	.88434	1.238	-1.17586	-1.13380	.00724	.87988	1.240
-1.0	-.93848	-.91217	.07218	.84615	1.469	-1.05479	-.90405	.04476	.83430	1.474	-1.17289	-.89977	.01514	.82664	1.478
-.8	-.91221	-.67008	.10612	.78459	1.718	-1.03719	-.65586	.07008	.76694	1.726	-1.16577	-.64731	.03073	.75398	1.736
-.6	-.86704	-.40999	.15403	.70603	1.988	-1.00376	-.38401	.10921	.68052	2.006	-1.14804	-.36578	.05981	.65934	2.020
-.4	-.78768	-.12936	.21902	.61175	2.284	-.93717	-.08079	.16719	.57666	2.322	-1.10228	-.04000	.10989	.54426	2.356
-.2	-.65094	.16372	.30213	.50700	2.612	-.80439	.25066	.24737	.46214	2.682	-.98400	.33932	.18743	.41714	2.762
-.1	-.55422	.30615	.34978	.45336	2.783	-.70055	.41620	.29560	.40434	2.884	-.87425	.53612	.23701	.35358	2.996
.1	-.30615	.55422	.45336	.34978	3.141	-.41620	.70055	.40434	.29560	3.296	-.53812	.87425	.35358	.23701	3.476
.2	-.16372	.65094	.50700	.30213	3.316	-.25066	.80439	.46214	.24737	3.494	-.33932	.98400	.41714	.18743	3.704
.4	.12936	.78768	.61175	.21902	3.642	.08079	.93717	.57666	.16719	3.856	.04000	1.10228	.54426	.10989	4.106
.6	.40999	.86704	.70603	.15403	3.938	.38401	1.00376	.68052	.10921	4.164	.36578	1.14804	.65934	.05981	4.440
.8	.67008	.91221	.78459	.10612	4.205	.65586	1.03719	.76694	.07008	4.446	.64731	1.16577	.75398	.03073	4.726
1.0	.91217	.93848	.84615	.07218	4.459	.90405	1.05479	.83430	.04476	4.700	.89977	1.17289	.82664	.01514	4.982
1.2	1.14091	.95423	.89220	.04875	4.688	1.13608	1.06457	.88434	.02869	4.936	1.13380	1.17586	.87988	.00724	5.220
1.4	1.36033	.96397	.92550	.03280	4.914	1.35736	1.07028	.92031	.01853	5.160	1.35608	1.17712	.91769	.00339	5.444
1.6	1.57359	.97012	.94900	.02203	5.127	1.57151	1.07374	.94558	.01207	5.376	1.57076	1.17767	.94401	.00157	5.662
1.8	1.78215	.97409	.96533	.01478	5.338	1.78095	1.07591	.96306	.00792	5.590	1.76049	1.17791	.96210	.00072	5.872
2.0	1.98804	.97667	.97654	.00991	5.548	1.98725	1.07728	.97503	.00523	5.800	1.98696	1.17801	.97443	.00033	6.084
2.2	2.19198	.97837	.98417	.00664	5.753	2.19147	1.07818	.98317	.00347	6.006	2.19128	1.17806	.98279	.00015	6.296
Exit	2.35619	.97846	.98836	.00568	5.916	2.35619	1.07870	.98764	.00252	6.170	2.35619	1.17815	.98738	.00008	6.460

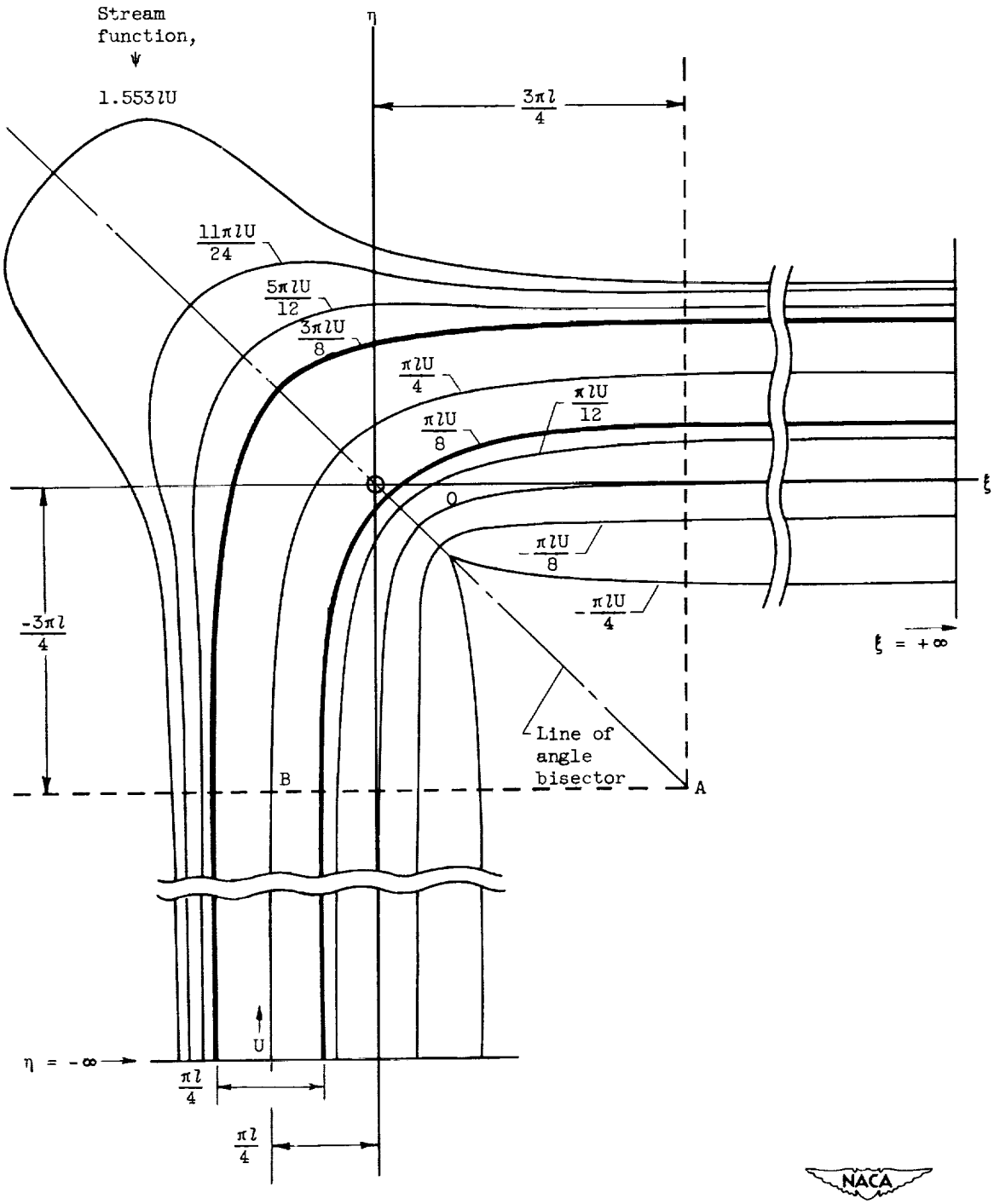

Figure 1. - Flow-field streamlines obtained from potential theory by equation (5).

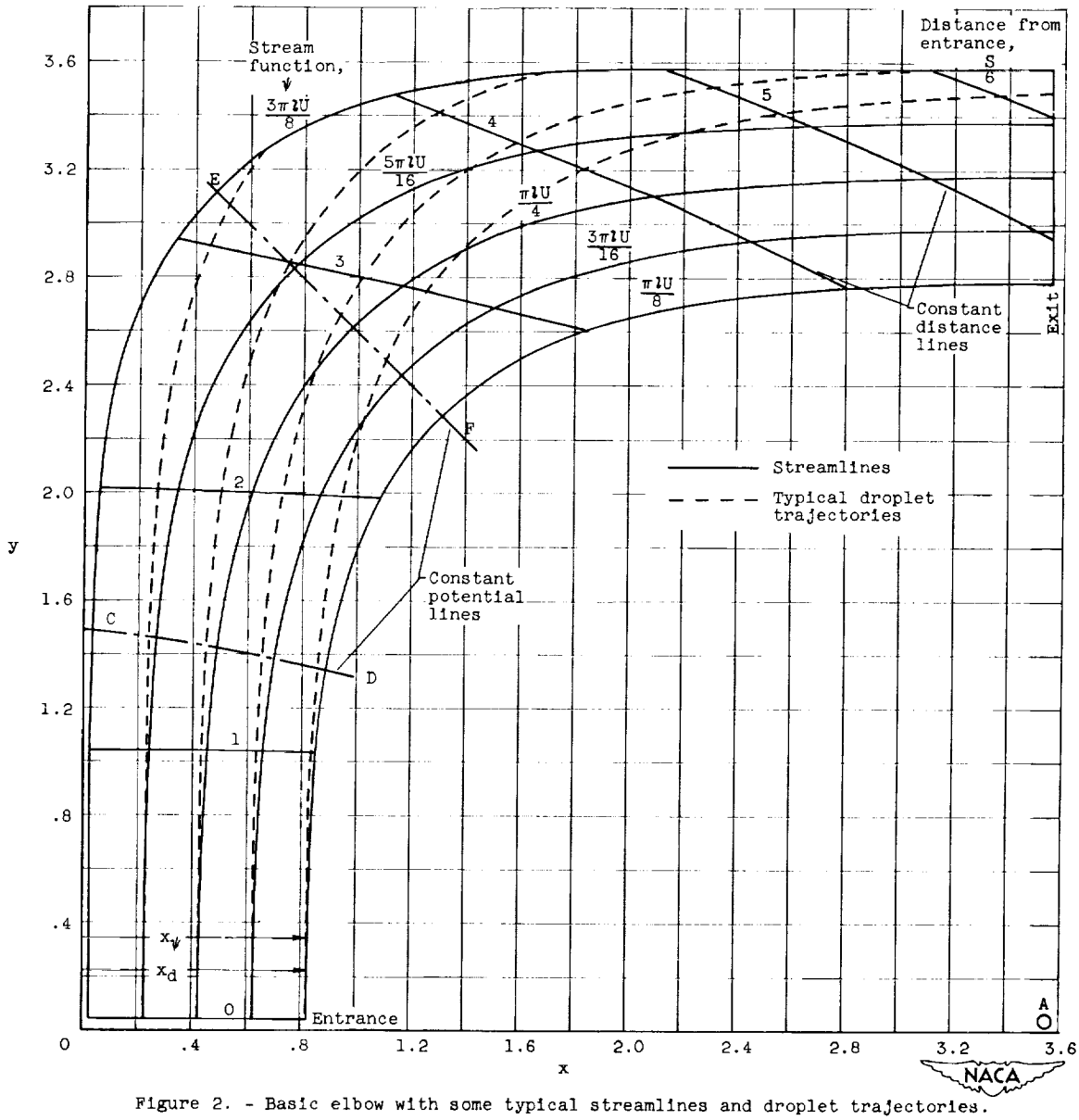

Figure 2. - Basic elbow with some typical streamlines and droplet trajectories.

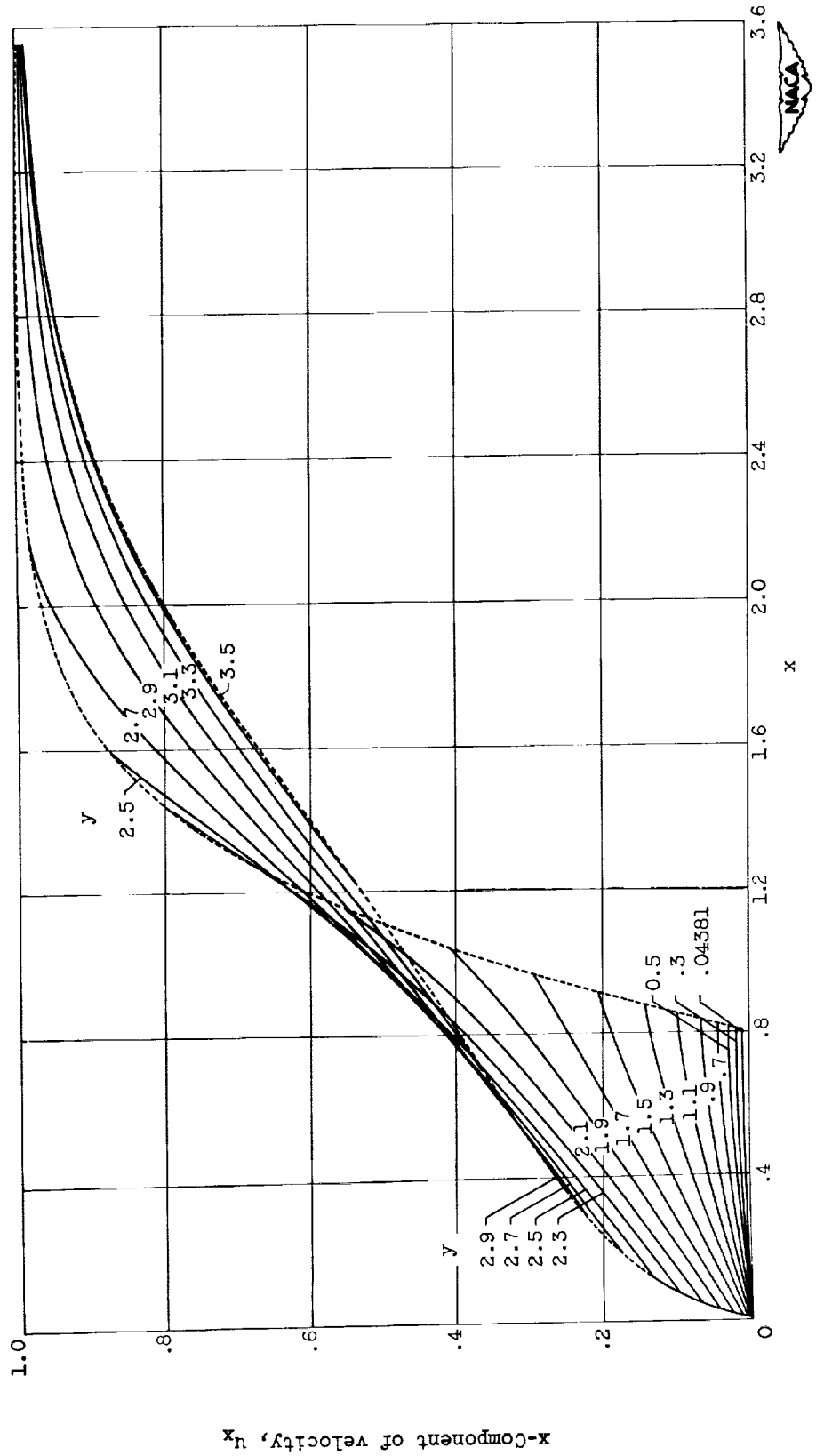

(a) x-Component of velocity.

Figure 3. - Elbow flow field.

2847

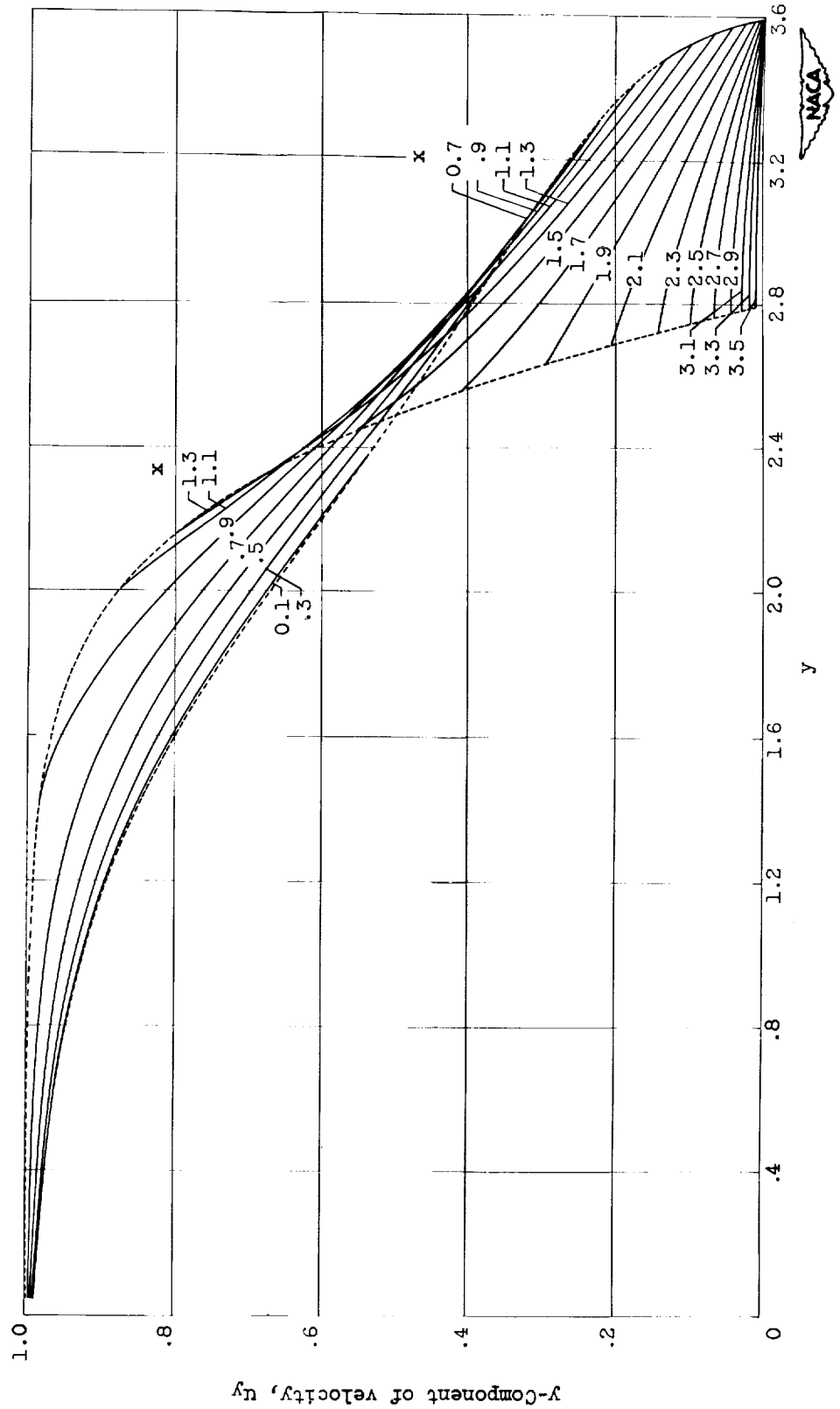

(b) y-Component of velocity.

Figure 3. - Concluded. Elbow flow field.

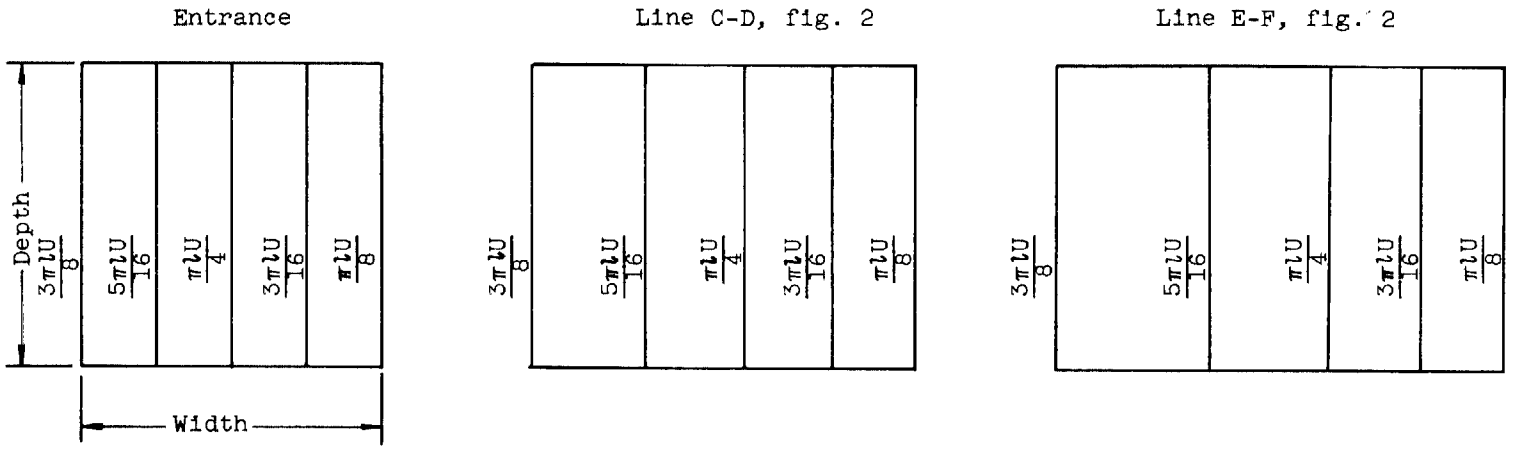

(a) Rectangular entrance.

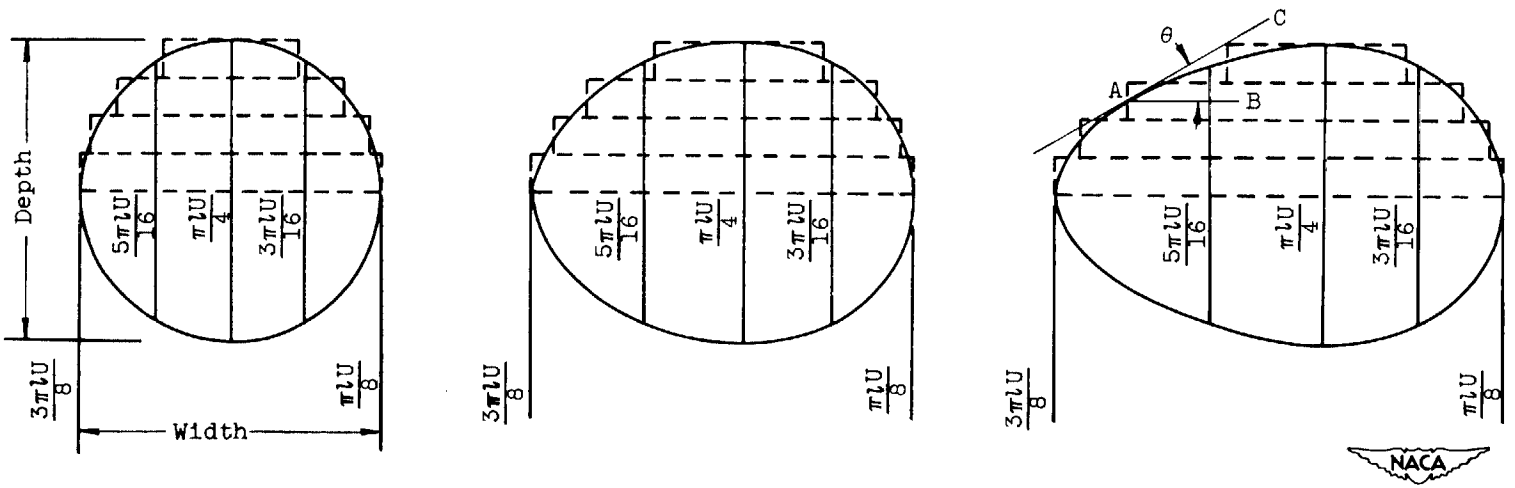

(b) Circular entrance.

Figure 4. - Typical cross sections of elbows with rectangular and circular entrances. Values shown are for stream function ψ.

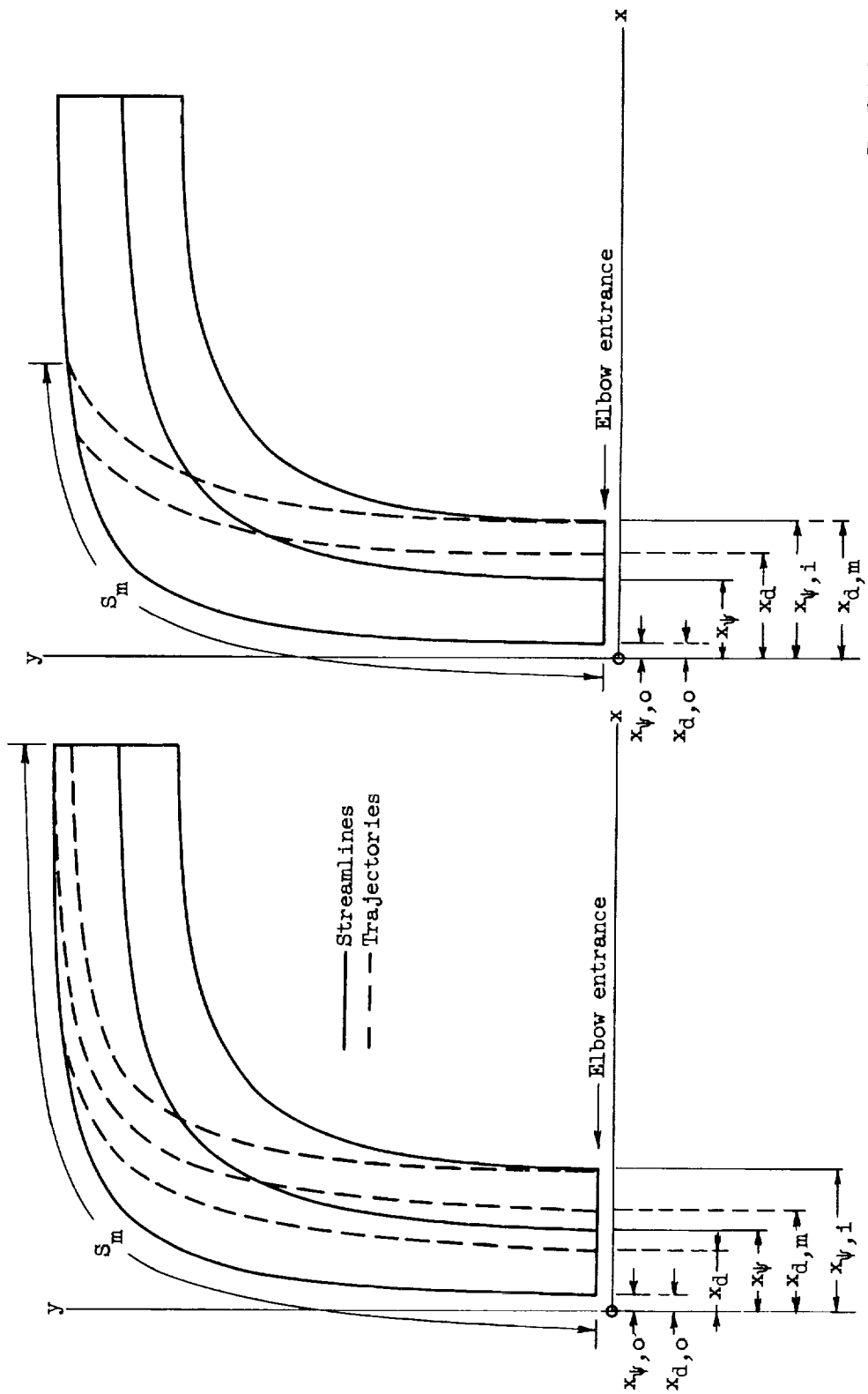

(a) Point of maximum extent of impingement at elbow exit.

(b) Point of maximum extent of impingement before elbow exit.

Figure 5. - Notation for streamlines and trajectories.

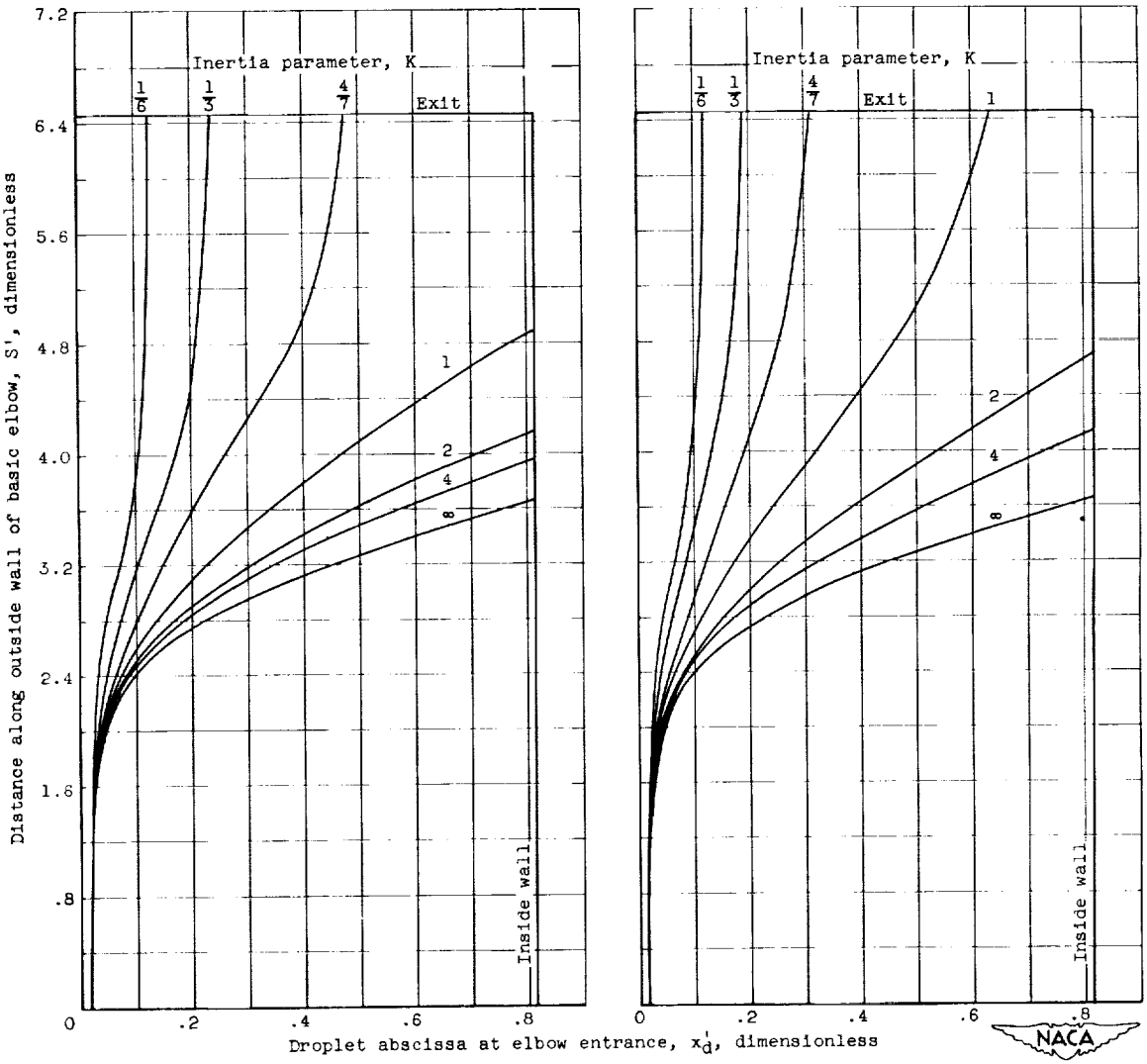

(a) Free-stream Reynolds number, 0. (b) Free-stream Reynolds number, 32.

Figure 6. - Point of droplet impingement on outside wall of basic elbow as function of droplet abscissa at elbow entrance.

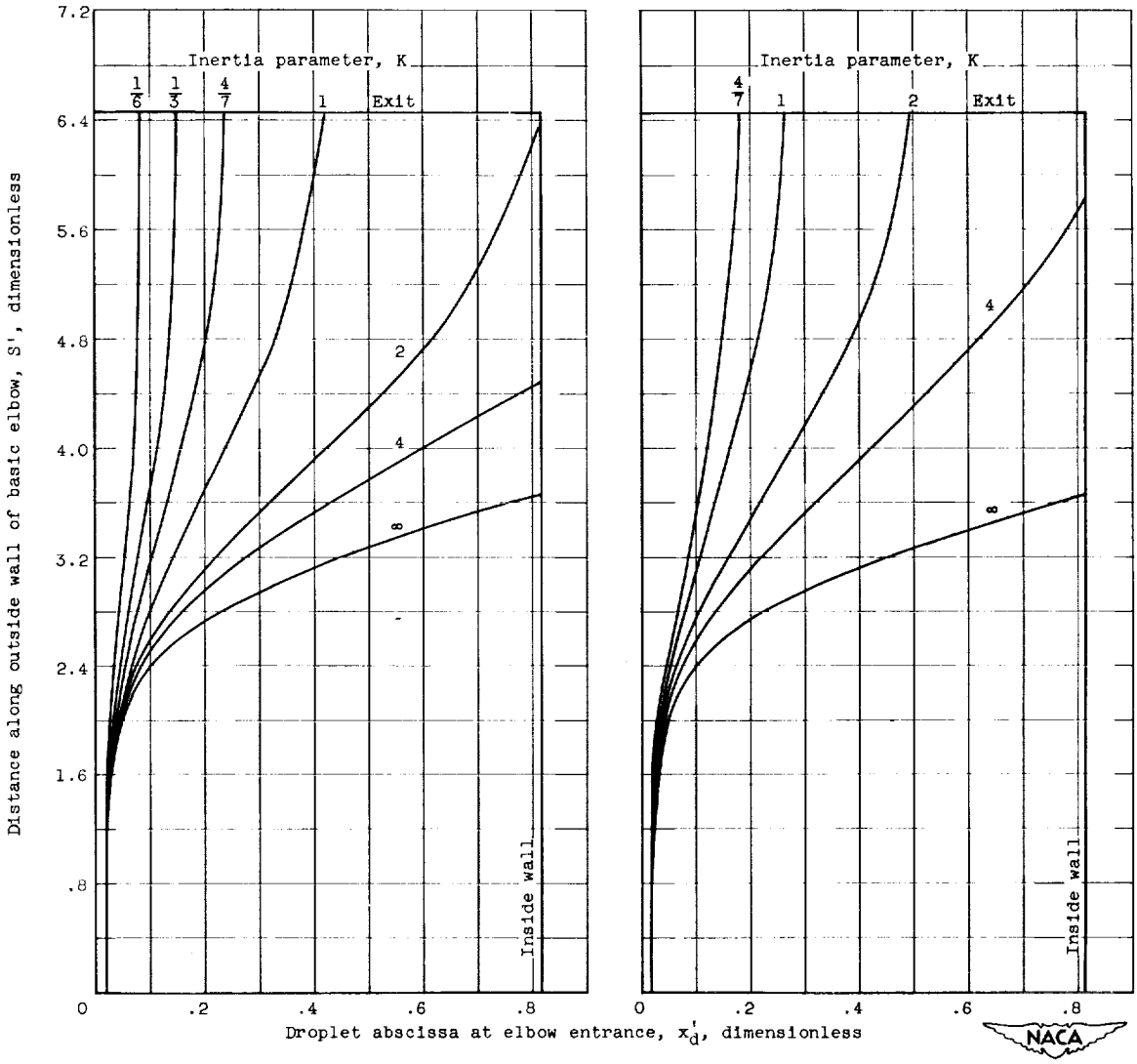

(c) Free-stream Reynolds number, 128. (d) Free-stream Reynolds number, 512.

Figure 6. - Concluded. Point of droplet impingement on outside wall of basic elbow as function of droplet abscissa at elbow entrance.

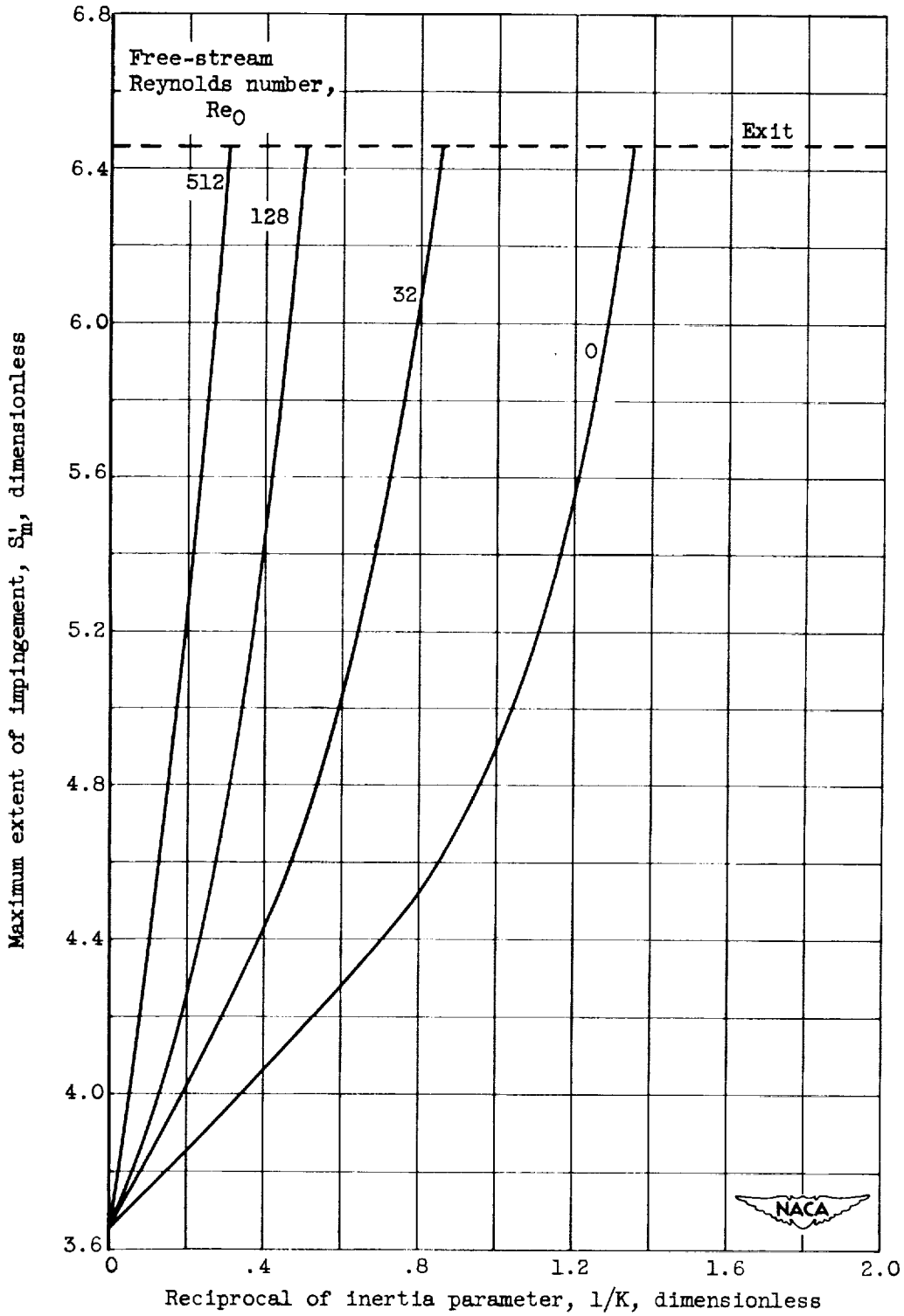

Figure 7. - Maximum extent of droplet impingement on outside wall of basic elbow as function of reciprocal of inertia parameter.

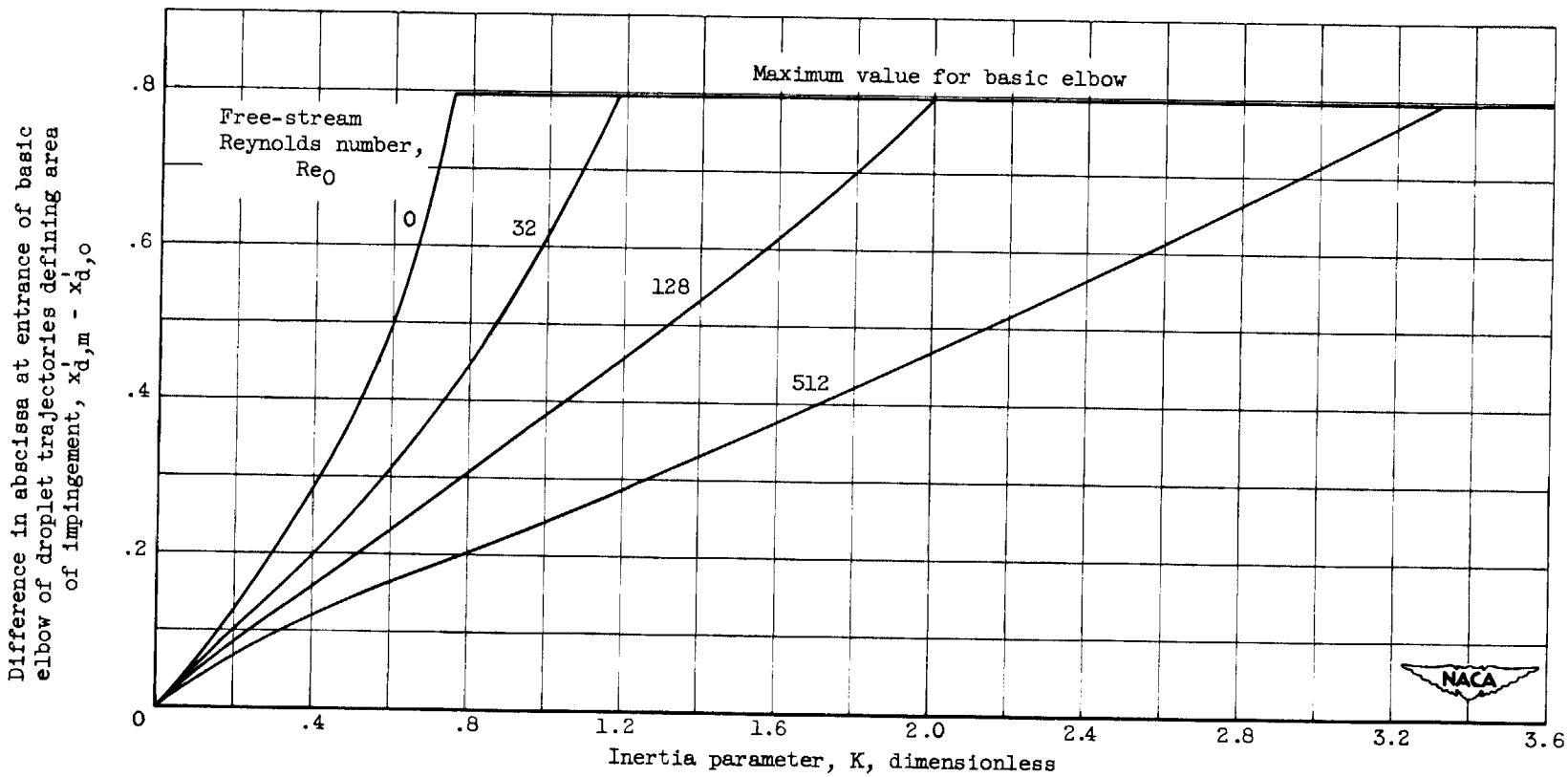

Figure 8. - Difference in abscissa at entrance of basic elbow of droplet trajectories defining area of impingement as function of inertia parameter.

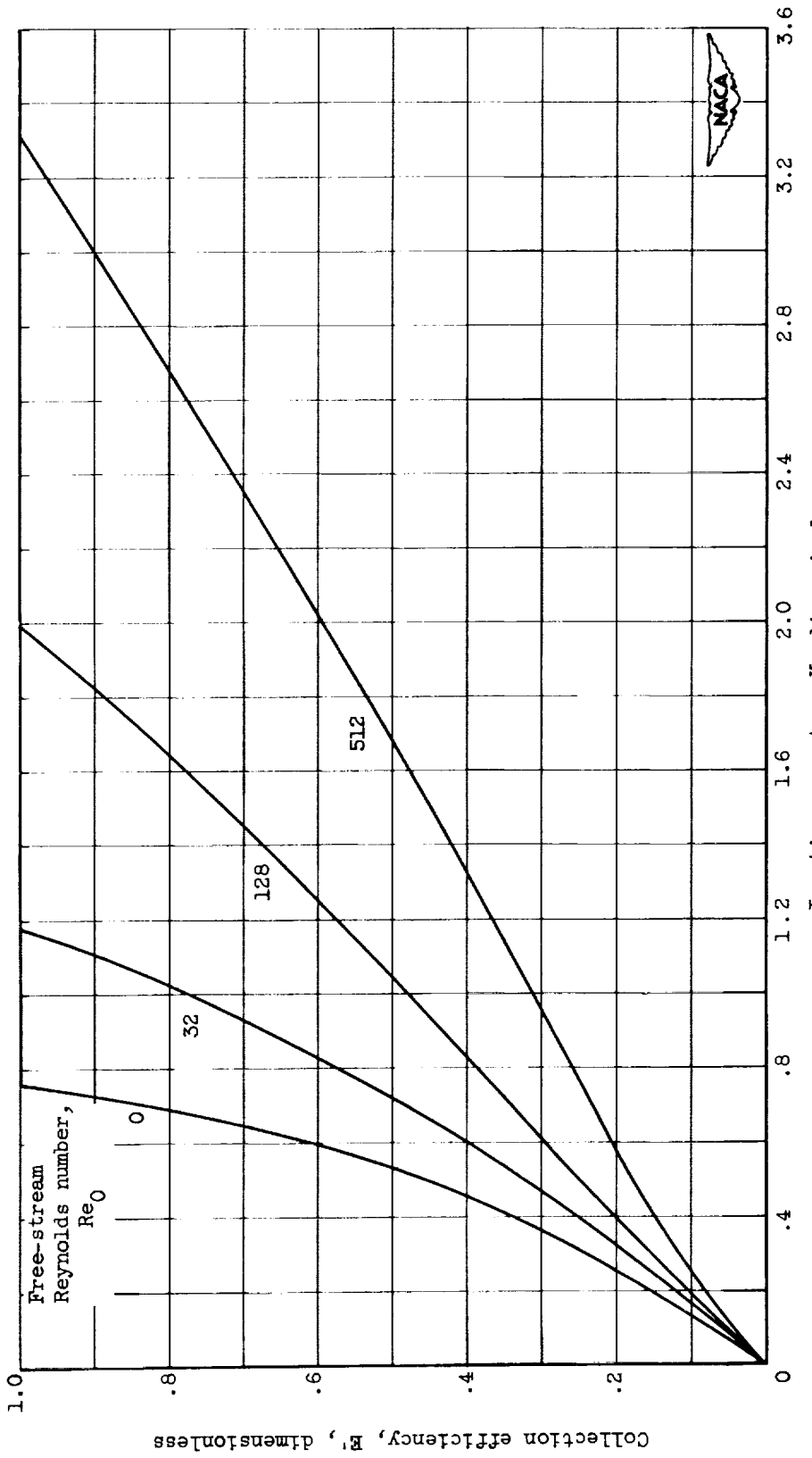

Figure 9. - Collection efficiency of basic elbow.

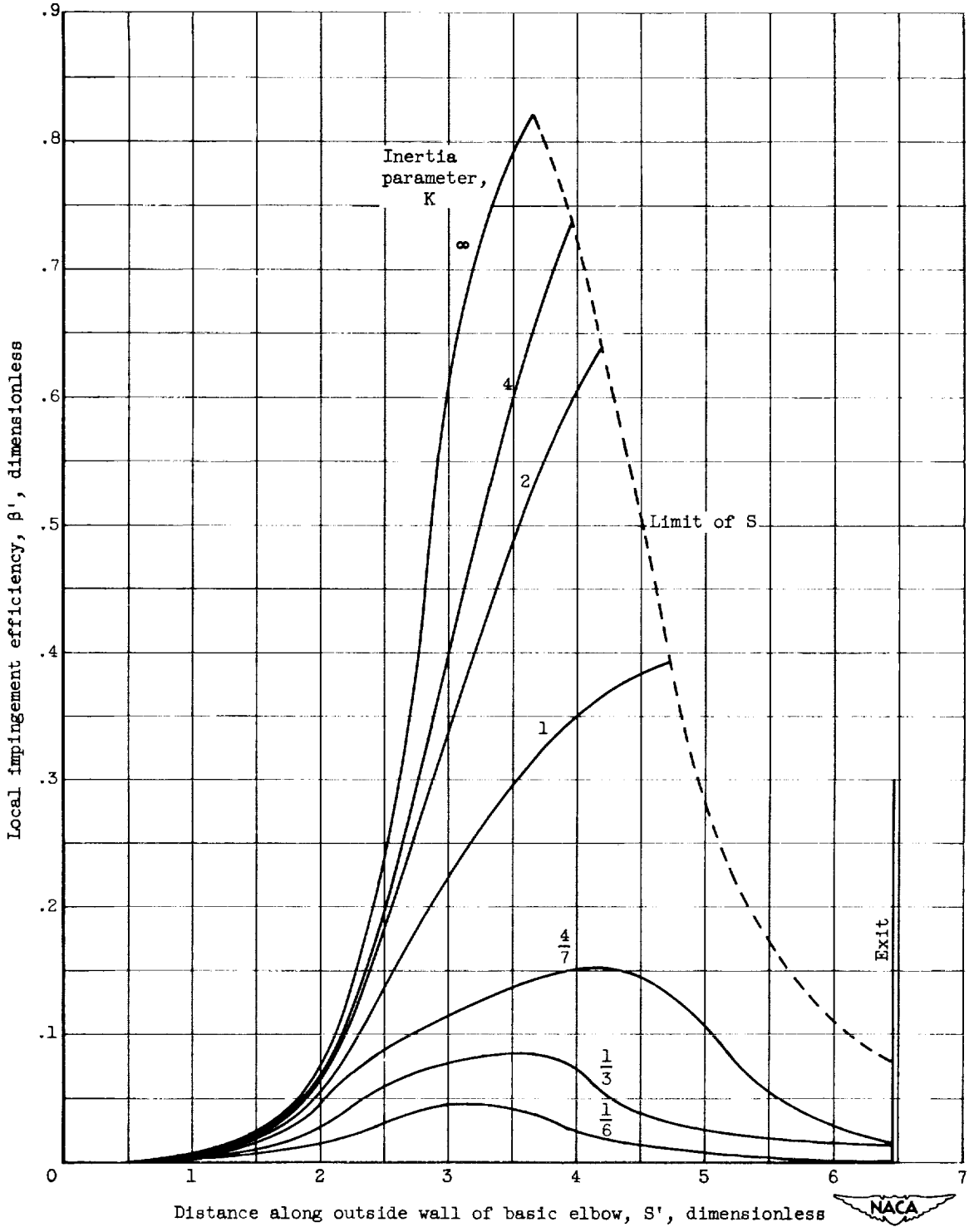

(a) Free-stream Reynolds number, O.

Figure 10. - Local impingement efficiency for basic elbow.

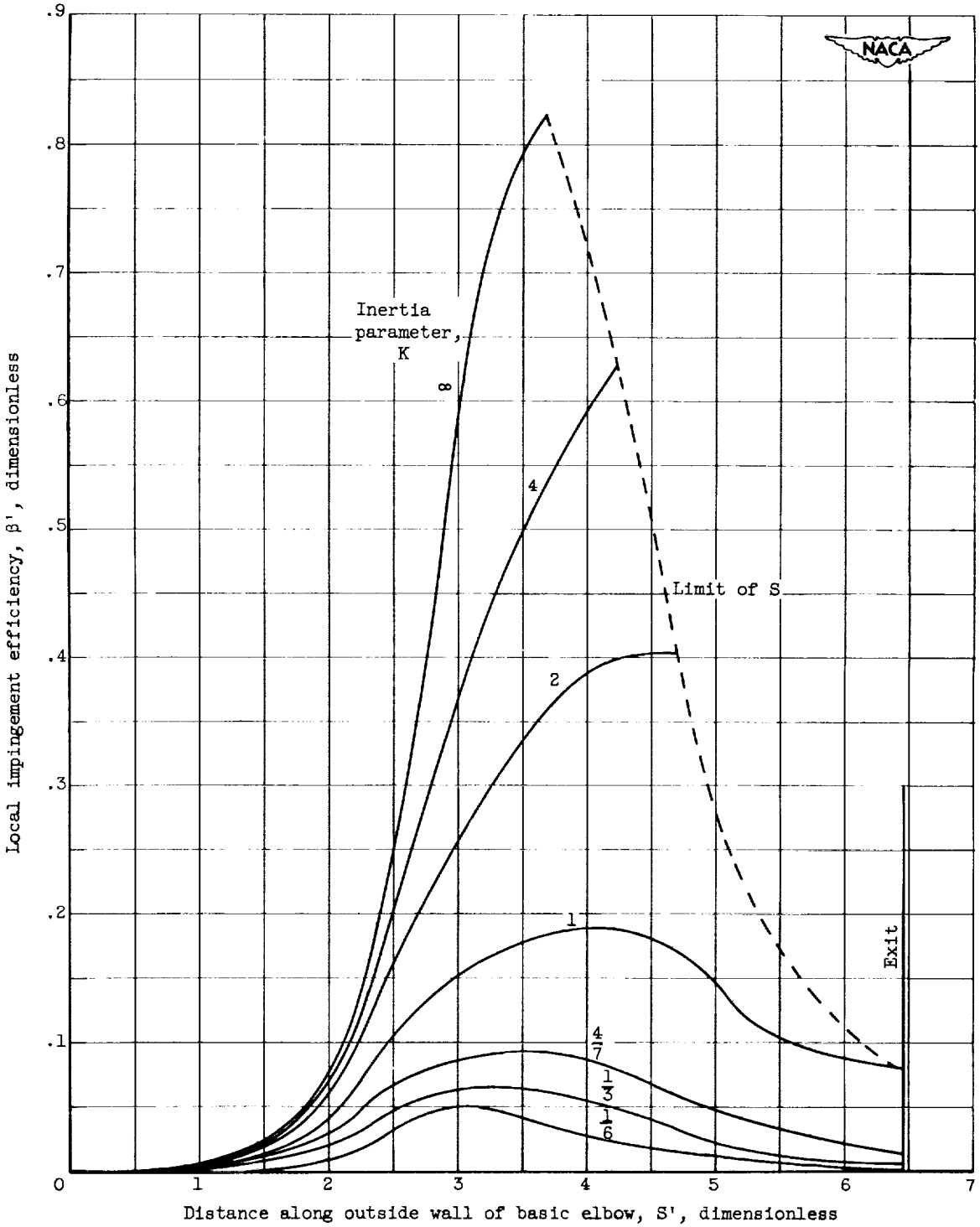

(b) Free-stream Reynolds number, 32.

Figure 10. - Continued. Local impingement efficiency for basic elbow.

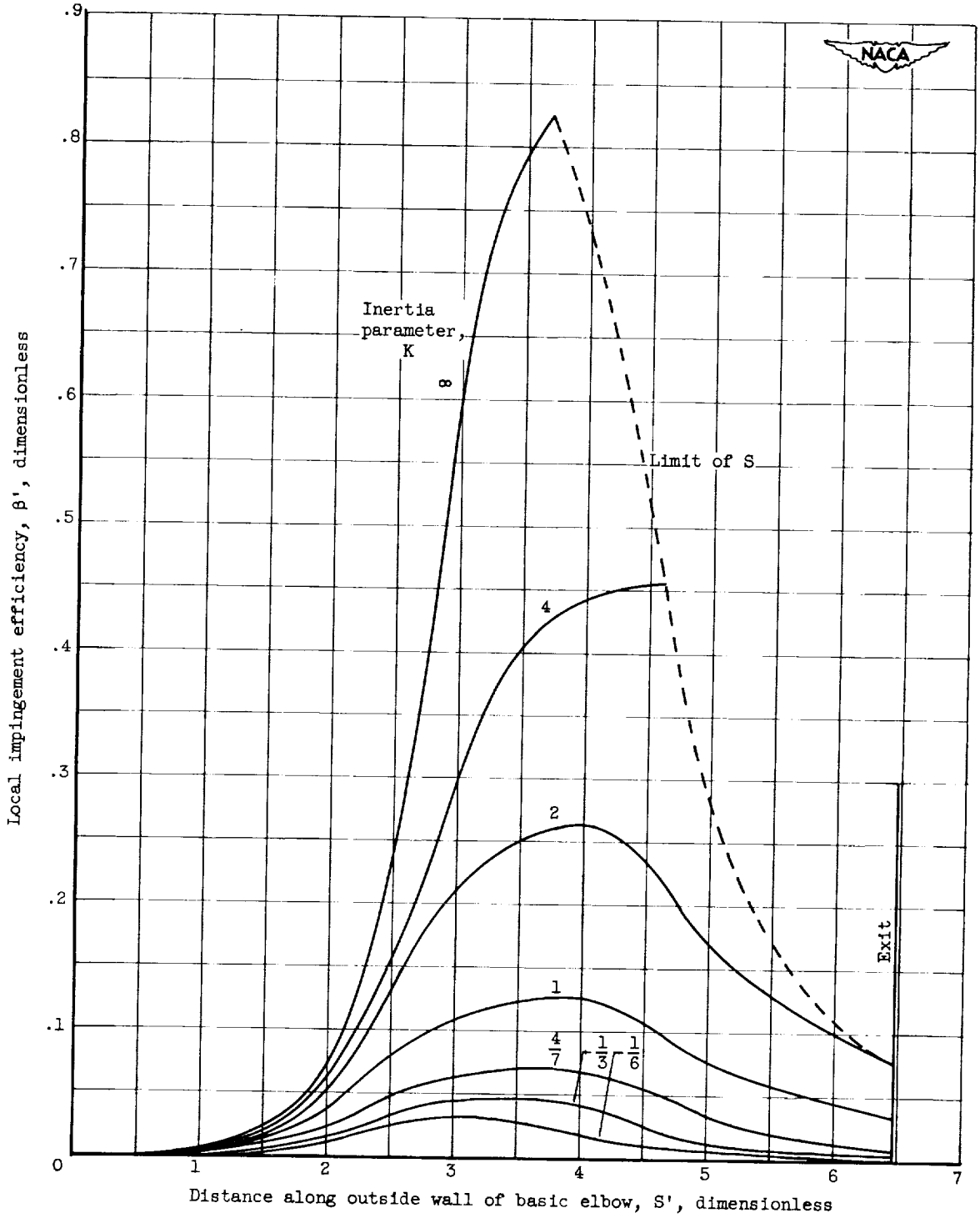

(c) Free-stream Reynolds number, 128.

Figure 10. - Continued. Local impingement efficiency for basic elbow.

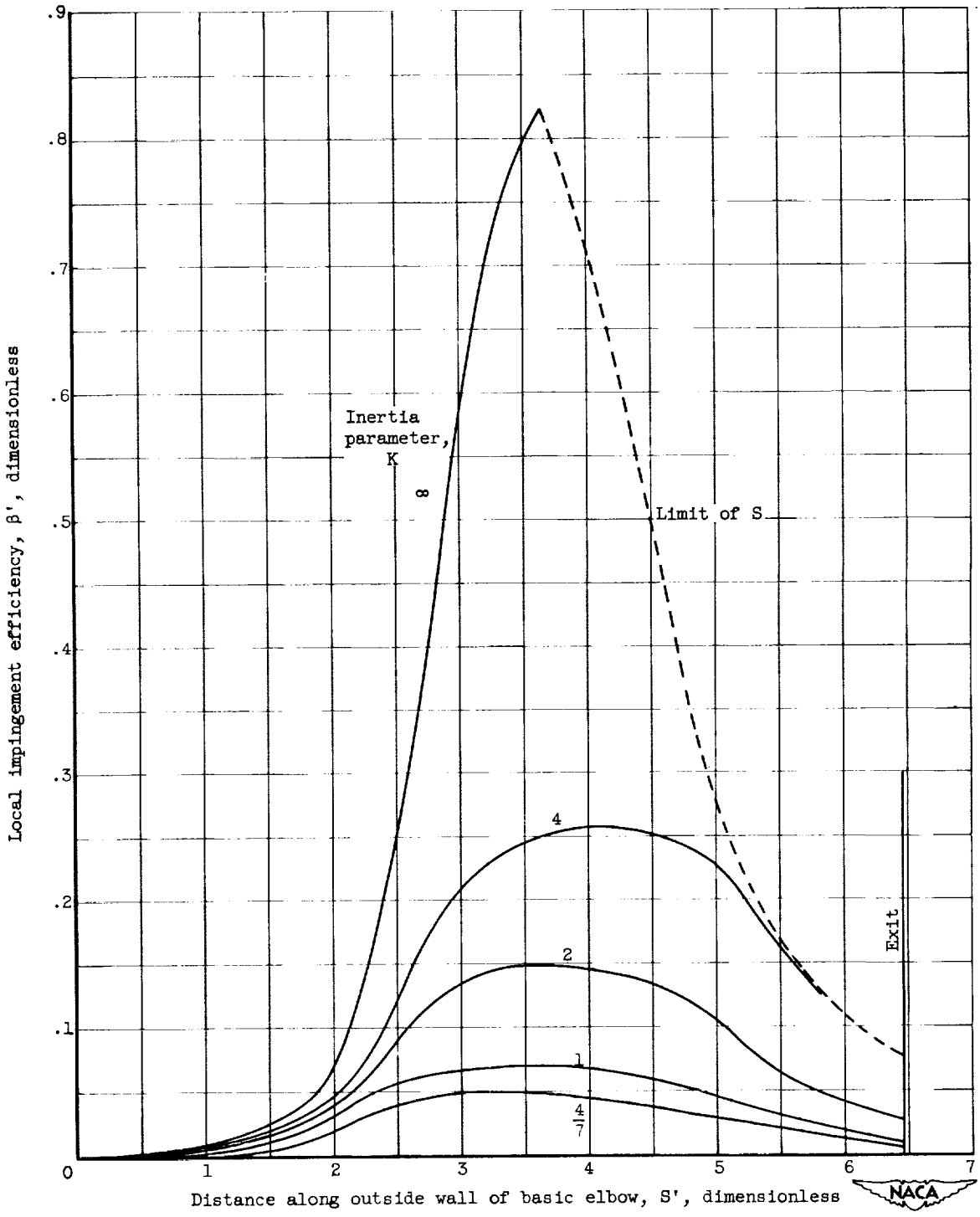

(d) Free-stream Reynolds number, 512.

Figure 10. - Concluded. Local impingement efficiency for basic elbow.

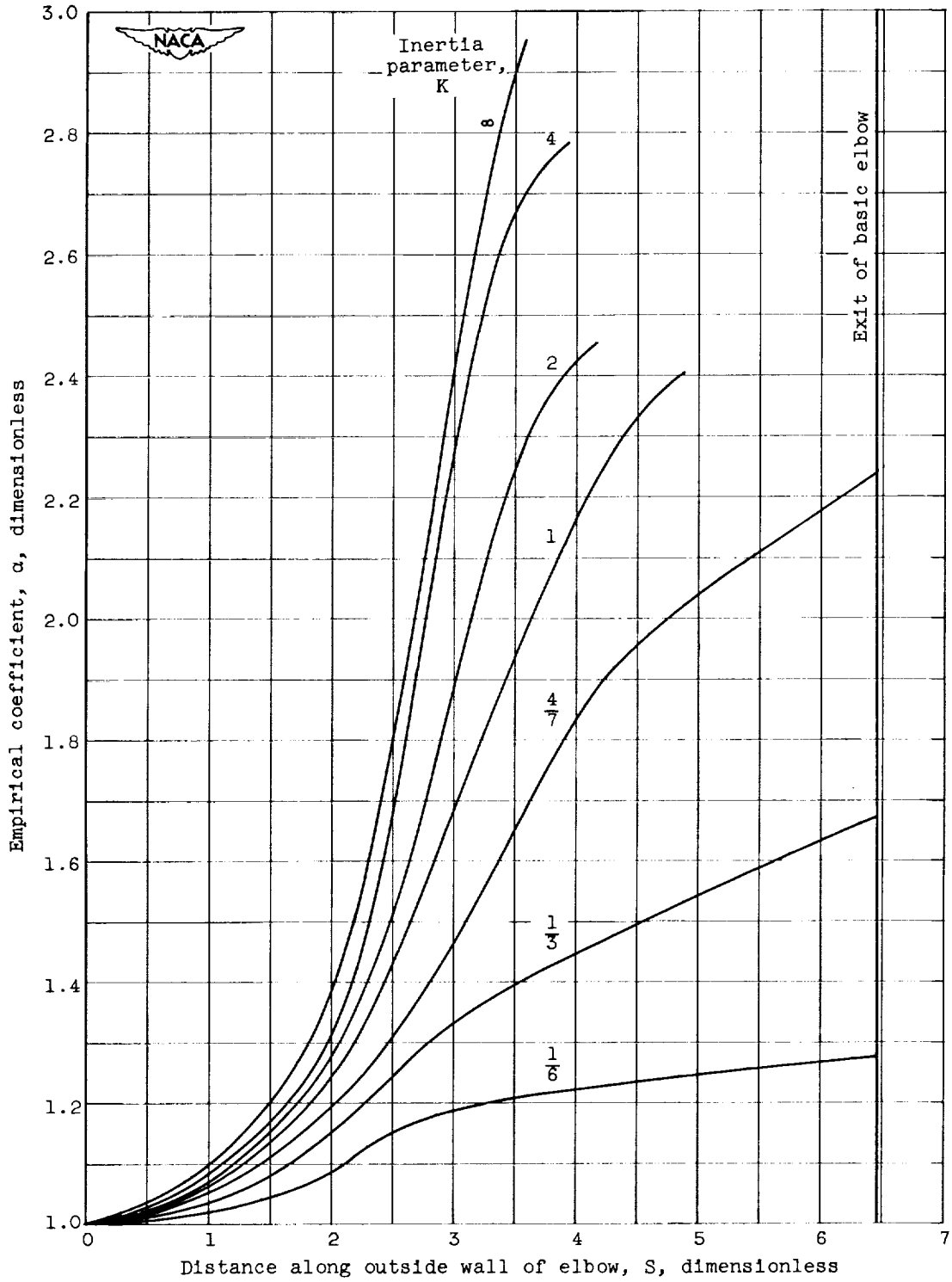

(a) Free-stream Reynolds number, O.

Figure 11. - Empirical coefficient for equation (13) as function of distance along outside wall of supplementary elbow.

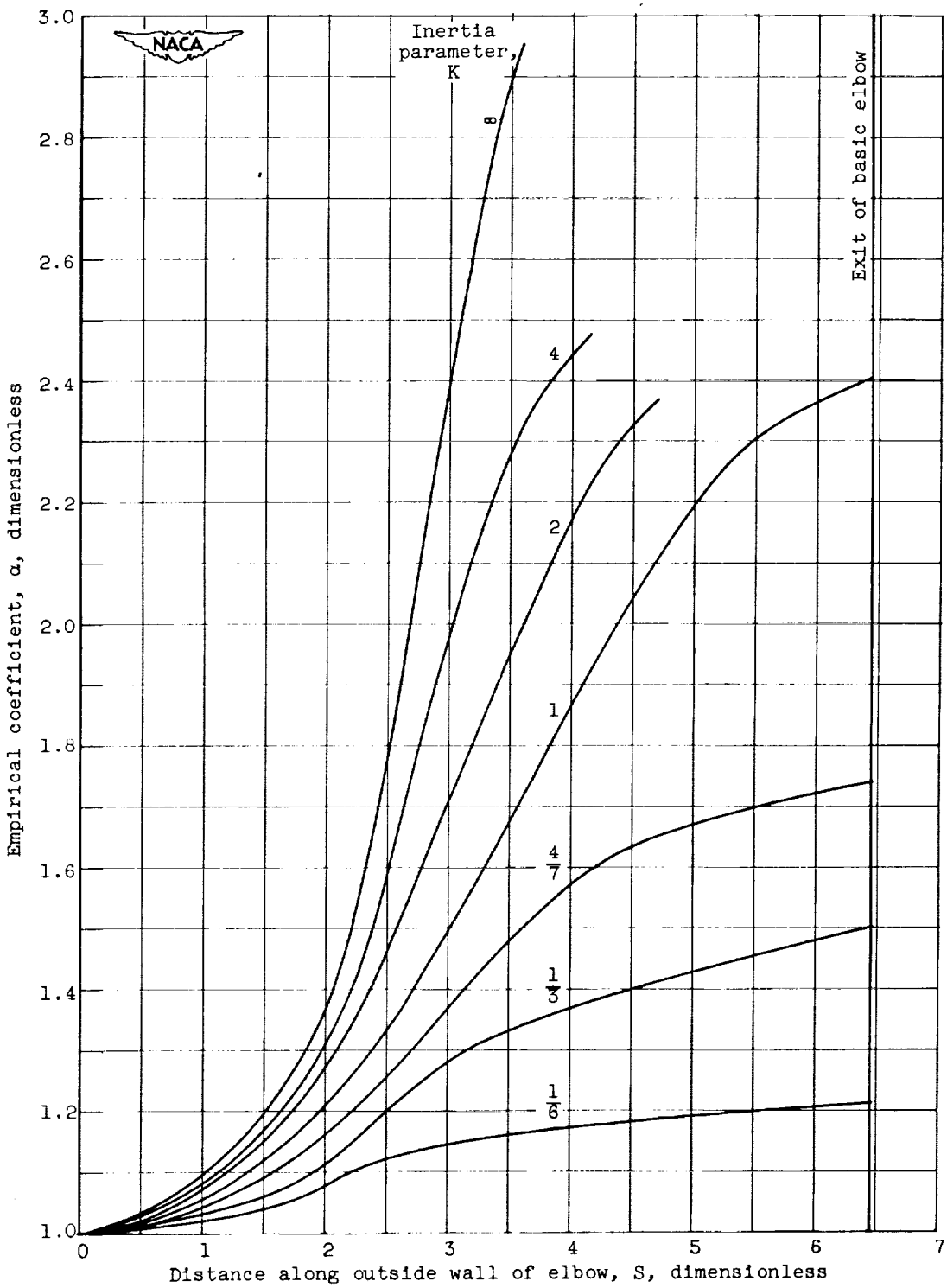

(b) Free-stream Reynolds number, 32.

Figure 11. - Continued. Empirical coefficient for equation (13) as function of distance along outside wall of supplementary elbow.

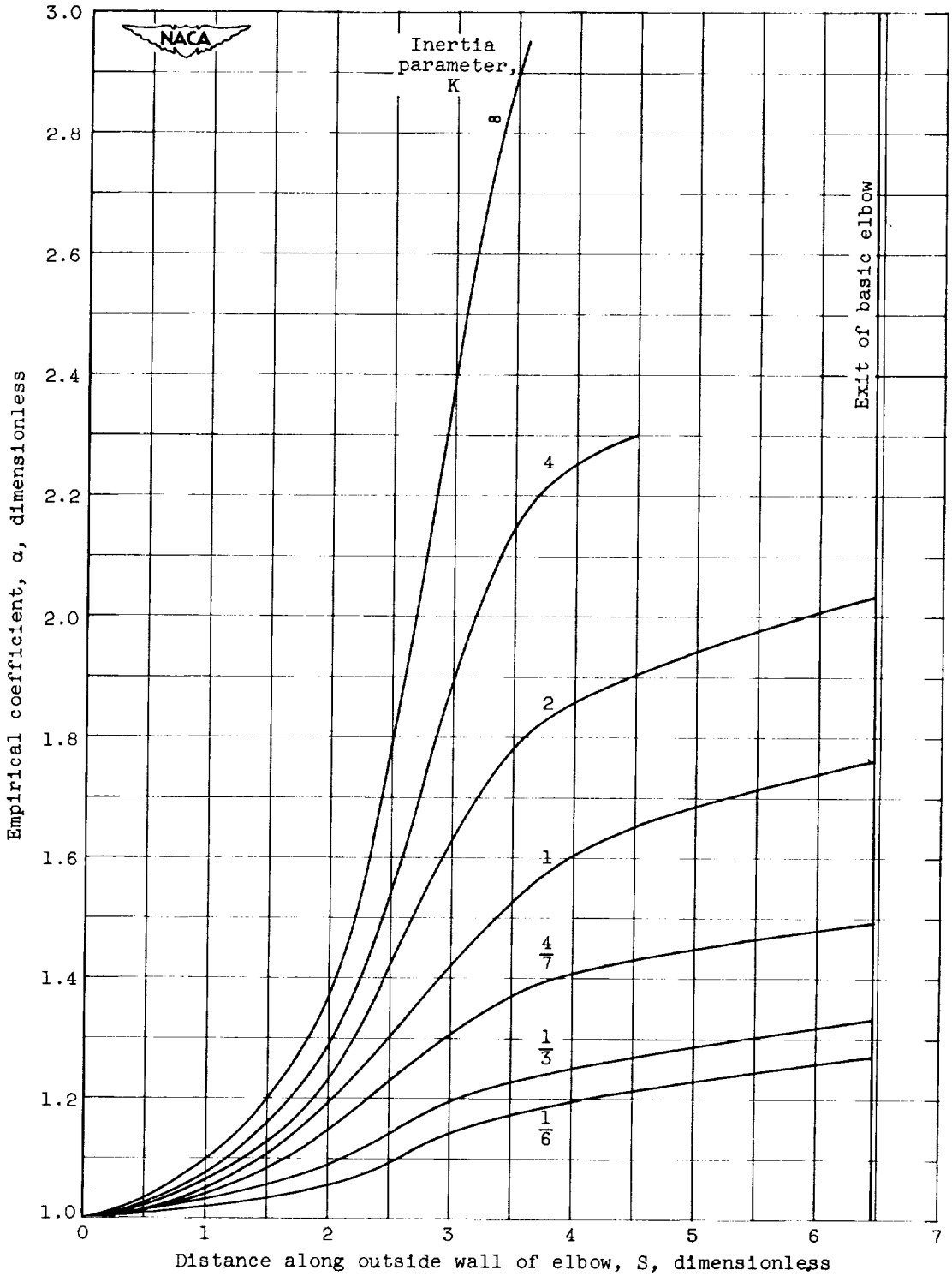

(c) Free-stream Reynolds number, 128.

Figure 11. - Continued. Empirical coefficient for equation (13) as function of distance along outside wall of supplementary elbow.

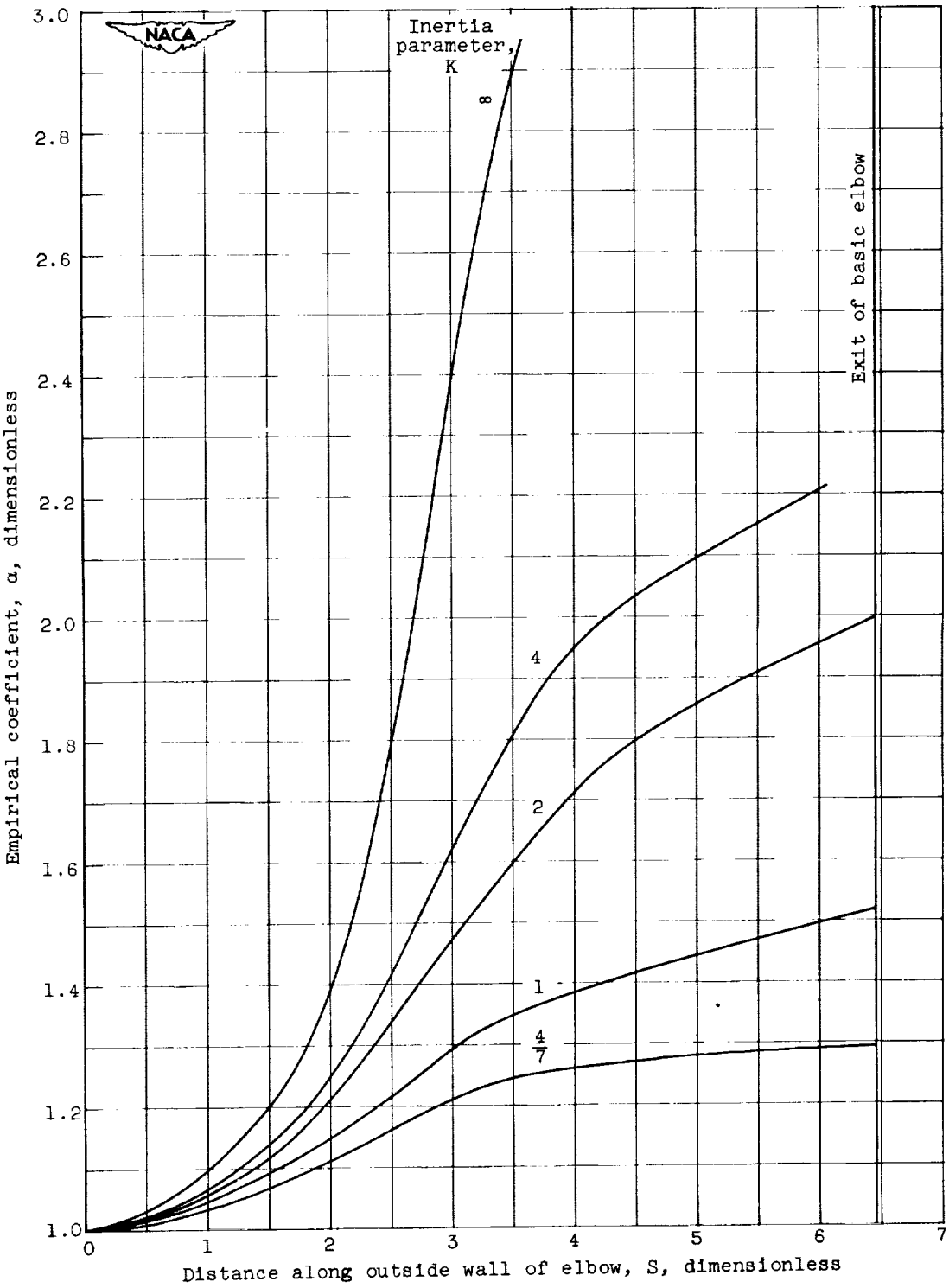

(d) Free-stream Reynolds number, 512.

Figure 11. - Concluded. Empirical coefficient for equation (13) as function of distance along outside wall of supplementary elbow.

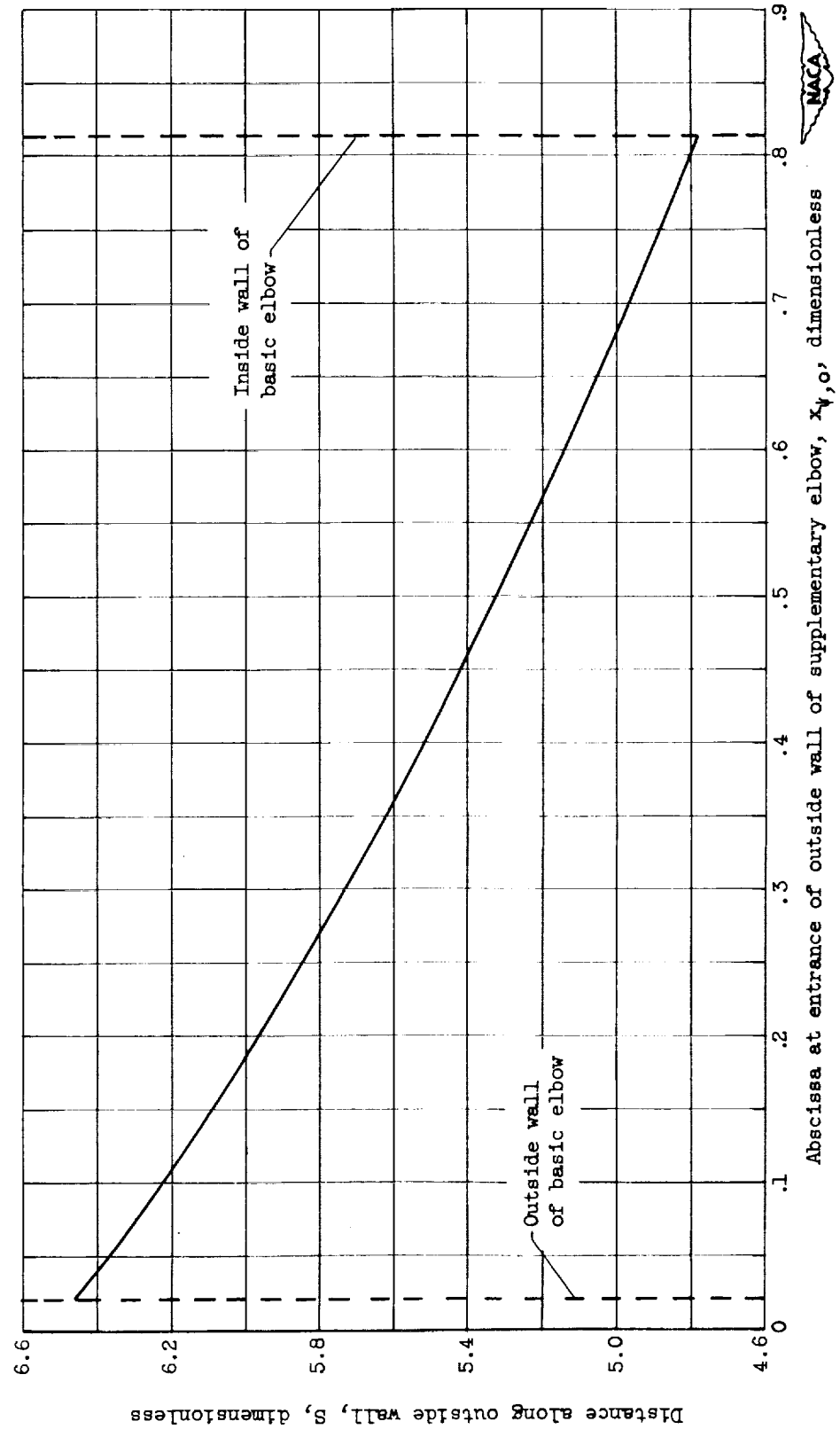

Figure 12. - Distance along outside wall at exit of supplementary elbows as function of abscissa value of outside wall at entrance.

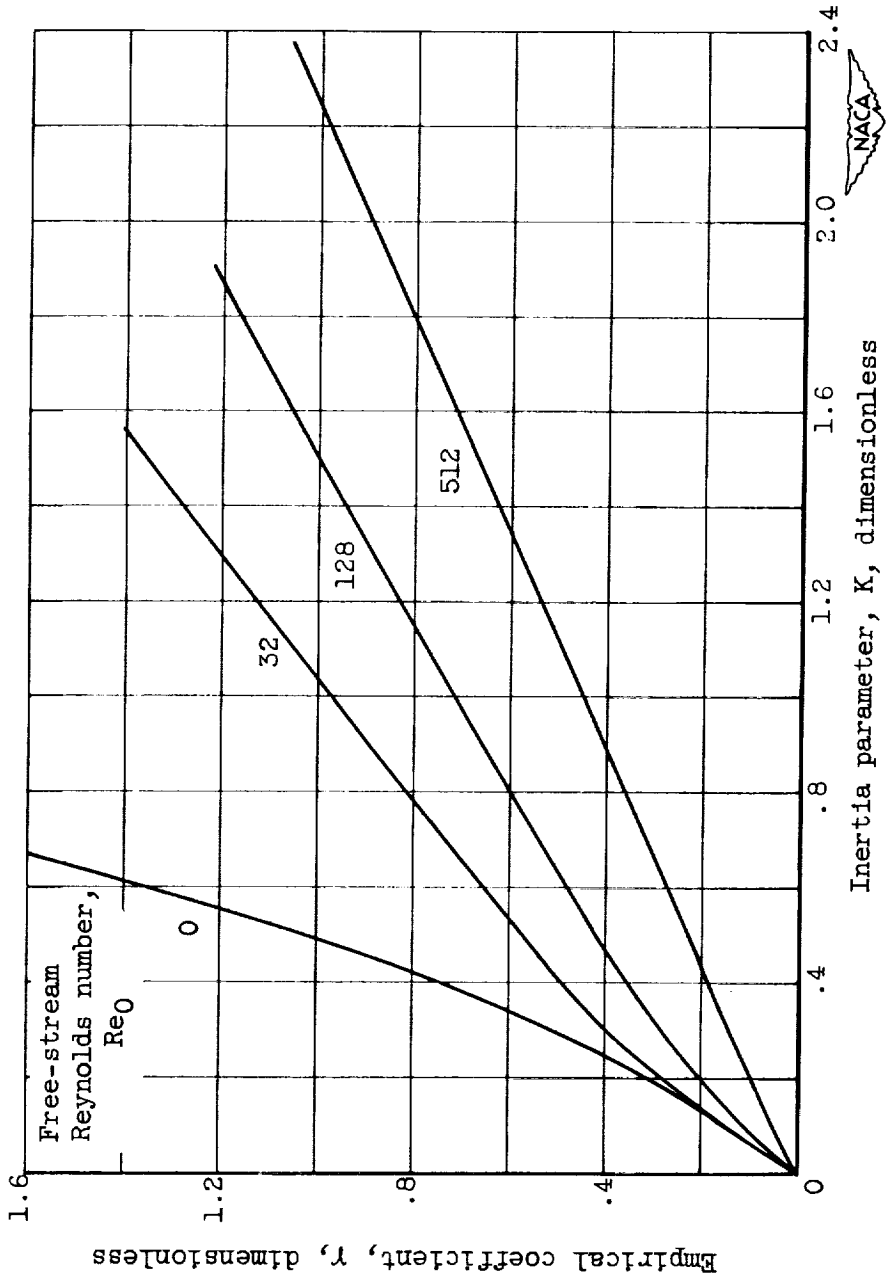

Figure 13. - Empirical coefficient for equation (15) as function of inertia parameter.

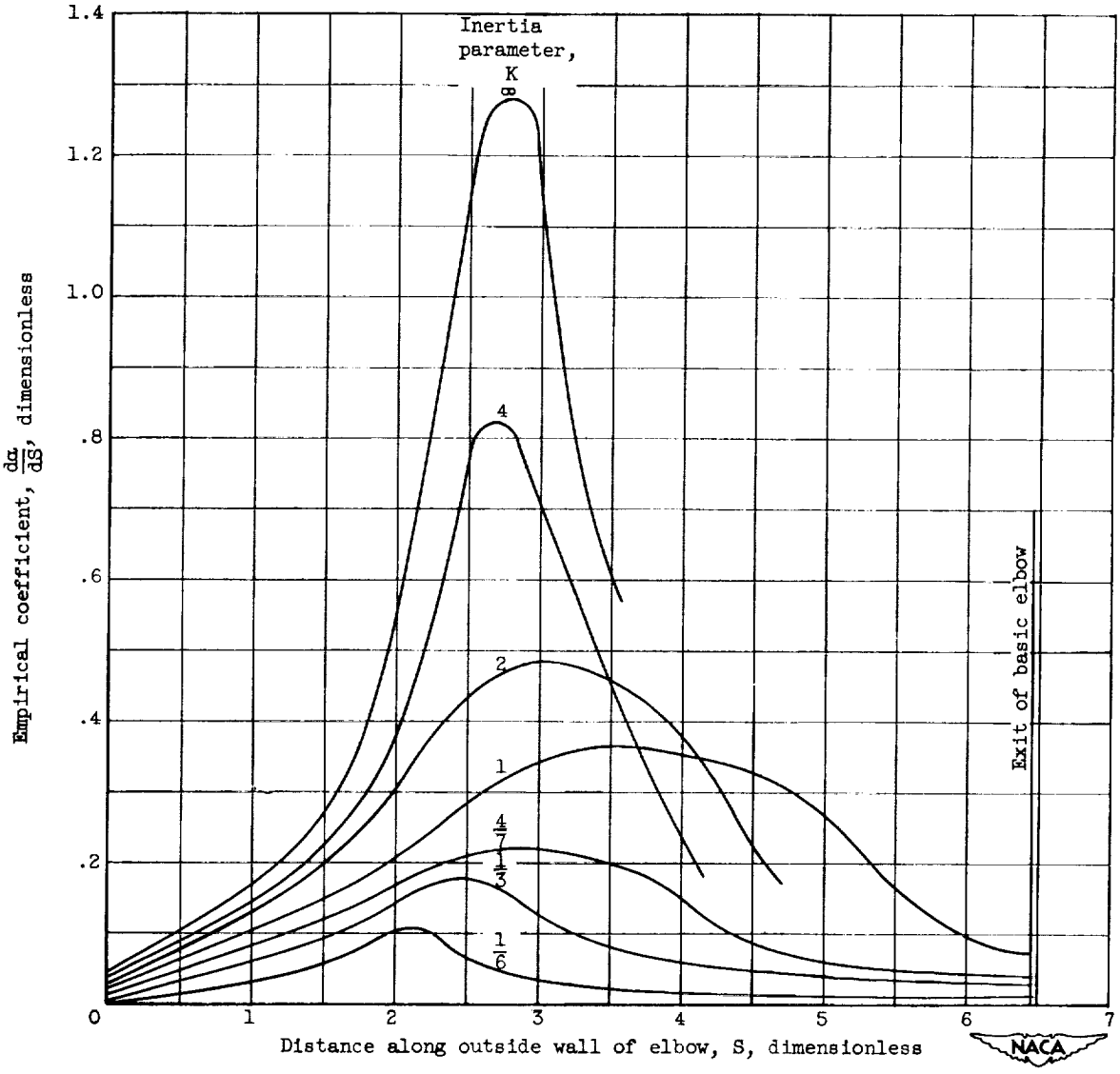

(b) Free-stream Reynolds number, 32.

Figure 14. - Continued. Empirical coefficient $\frac{d\alpha}{dS}$ for equation (21) as function of distance along outside wall of supplementary elbow.

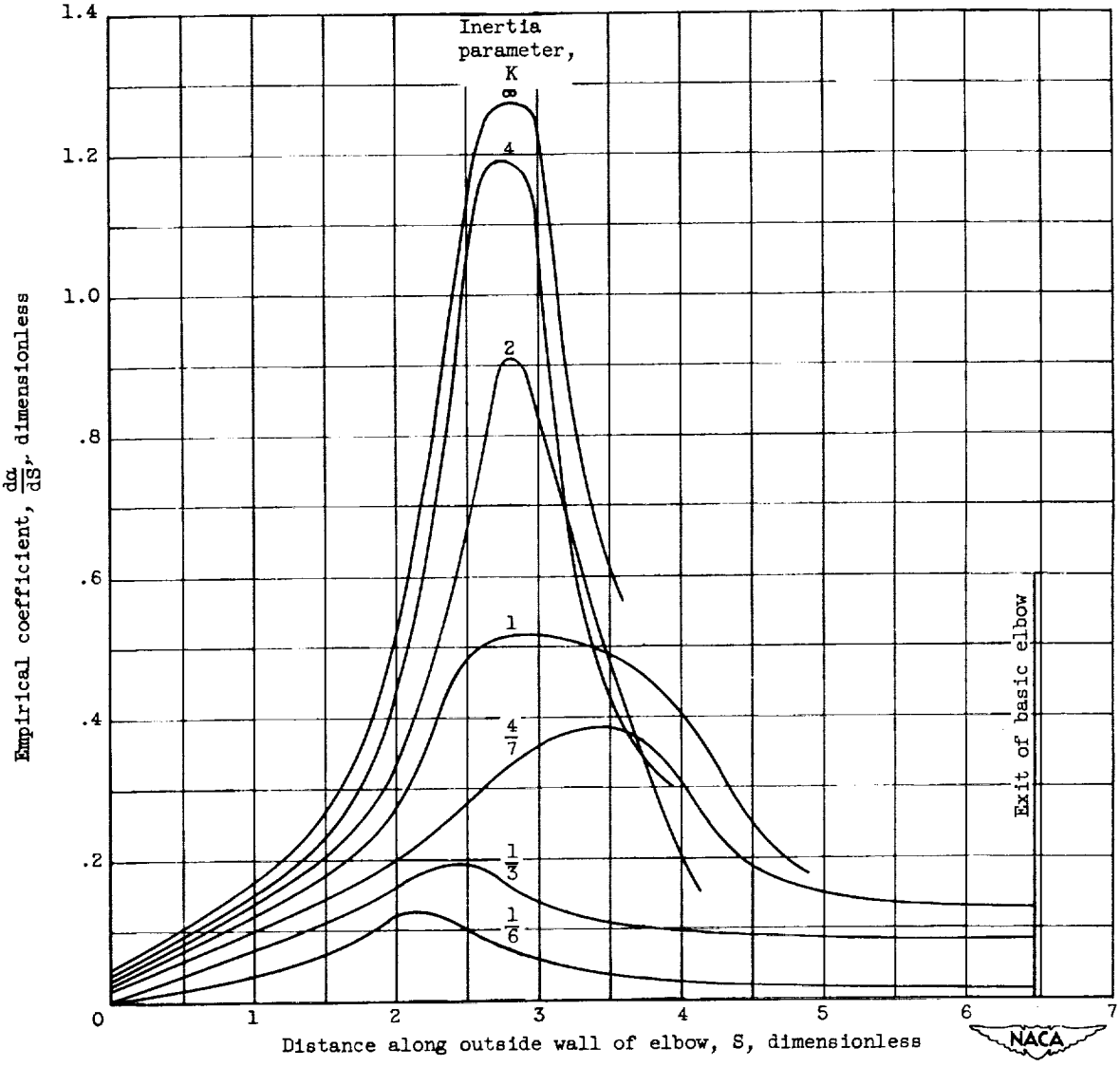

(a) Free-stream Reynolds number, O.

Figure 14. - Empirical coefficient $\frac{d\alpha}{dS}$ for equation (21) as function of distance along outside wall of supplementary elbow.

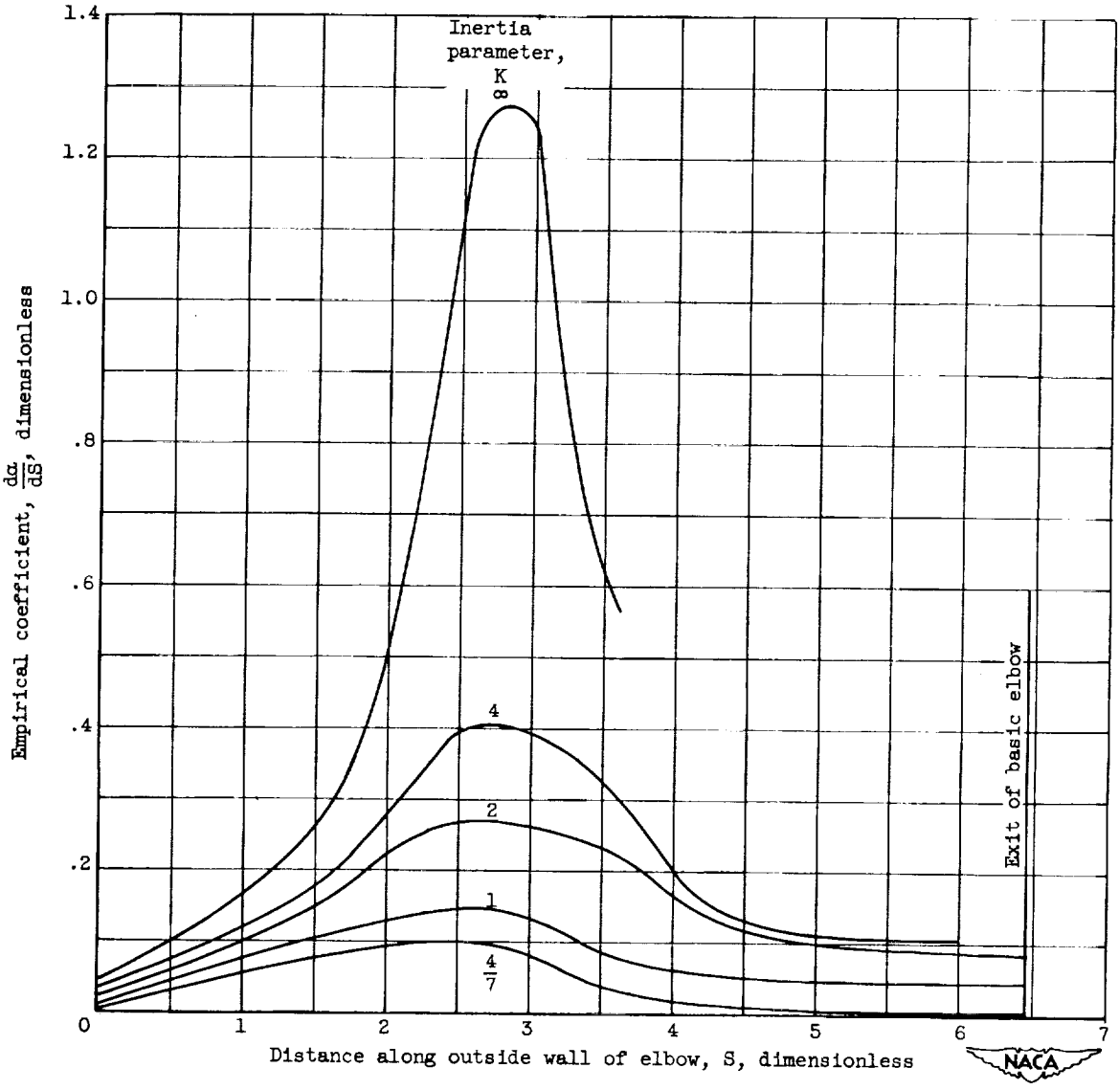

(d) Free-stream Reynolds number, 512.

Figure 14. - Concluded. Empirical coefficient $\frac{d\alpha}{dS}$ for equation (21) as function of distance along outside wall of supplementary elbow.

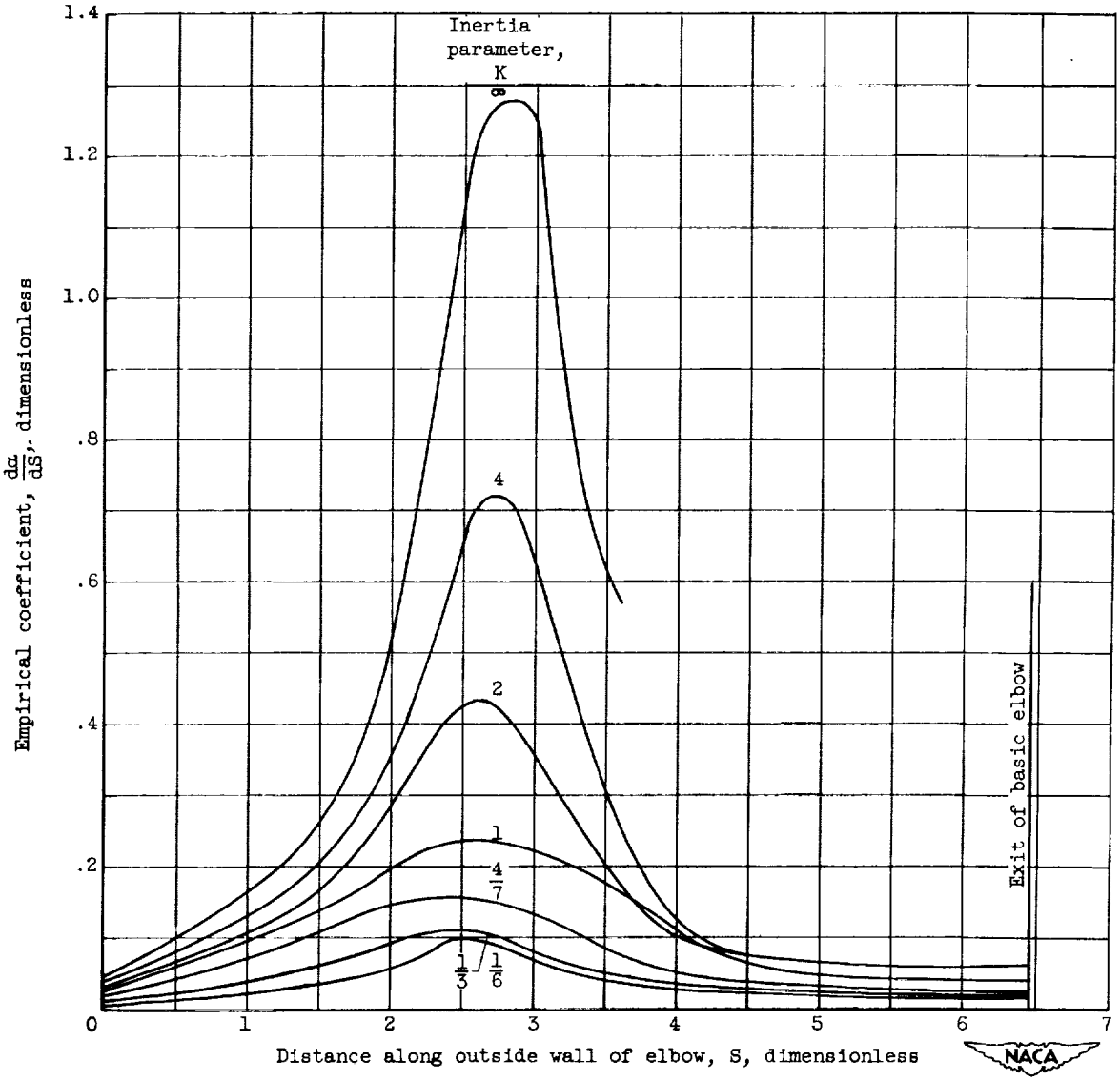

(c) Free-stream Reynolds number, 128.

Figure 14. - Continued. Empirical coefficient $\frac{d\alpha}{dS}$ for equation (21) as function of distance along outside wall of supplementary elbow.